Utilization of Floral waste for hydrogen generation via photocatalytic water splitting

THESIS

SUBMITTED IN THE PARTIAL FULFILLMENT OF THE REQUIREMENT FOR THE DEGREE OF

MASTER OF ENGINEERING

BY

PAWAN KUMAR

ROLL-NO: 002210302010

Registration No-163439

Exam Roll No- M4CHE24010

Academic Seasons-2022-2024

Under

Prof. KAJARI KARGUPTA

CHEMICAL ENGINEERING DEPARTMENT

JADAVPUR UNIVERSITY

KOLKATA – 700032, WEST BENGAL

Faculty of Engineering and Technology
Jadavpur University

Certificate

This is to certify that Mr. Pawan Kumar, a Final year Master of Chemical Engineering student of the Department of Chemical Engineering, Jadavpur University, Class Roll No. 002210302010, Registration No. 163439 of 2022-2023 has completed Project work titled, "**Utilization of Floral waste for hydrogen generation via photocatalytic water splitting**" under the guidance of **Prof. Kajari Kargupta** during his Master's Curriculum. This work has not been reported earlier anywhere and can be approved for submission in partial fulfillment of the coursework.

.....

Prof. Papita Das

Head of the Department

Chemical Engineering Department

Jadavpur University

Kajari Kargupta 31/05/2024

Prof. Kajari Kargupta

Project Supervisor

Chemical Engineering Department

Jadavpur University

Professor
CHEMICAL ENGINEERING DEPARTMENT
JADAVPUR UNIVERSITY
Kolkata-700 032

Dipak Laha 31/5/24

Signature of the Dean

Faculty of Engineering and Technology

Jadavpur University Kolkata – 700032

Place – Kolkata

Date – 31 May 2024

DEAN
Faculty of Engineering & Technology
JADAVPUR UNIVERSITY
KOLKATA-700 032

Declaration

I hereby declare that the contents of this thesis are composed of original research work and a literature review by the undersigned as a part of Master of Chemical Engineering (Department of Chemical Engineering) studies. The information in this document is by ethical conduct and the academic rules.

I also declare that I have cited all the references for the material that are not original to this work.

Pawan Kumar
21/05/2024

.....

Place – Kolkata

Date – 31 May 2024

Pawan Kumar

Roll No.- 002210302010

Exam Roll No.- M4CHE24010

Master of Chemical Engineering

Chemical Engineering Department

Jadavpur University

This thesis is dedicated to

my beloved parents

For their constant love, support, and encouragement

Acknowledgment

I want to express my sincere gratitude to my guide, **Prof. Kajari Kargupta**, for her unwavering support and guidance throughout this research project. Her expertise, encouragement, and patience have been invaluable, and I could not have completed this work without her assistance.

I am incredibly grateful to **Prof. Papita Das**, Head of the Chemical Engineering Department, for all the help I got during my project work.

I would also like to thank my lab mates at NSEL, **Mr. Sayantanu Mandal**, **Ms. Arundhati Sarkar**, **Mr. Arindam Mandal**, and **Ms. Swagata Das** for their collaboration, feedback, and support. Their insights and contributions were crucial to the success of this project, and I am grateful for their willingness to share their time and knowledge with me.

In addition, I would like to thank our lab assistant of NSEL, **Mr. Ajay Kr. Pradhan**, for his assistance with the practical aspects of this project. His help with laboratory experiments and equipment maintenance made a significant difference in the quality and accuracy of our results. I am also indebted to Jadavpur University, Dept. of Chemical Engineering, for supporting me and allowing me to use the equipment to do my research.

Finally, I would like to acknowledge the support of my mother **Mrs. Kiran Devi**, my father **Mr. Ashok Saw**, and friends who have encouraged me throughout my academic journey and provided me with the emotional and logistical support necessary to complete this project.

Thank you all for your contributions to this work.

Pawan Kumar
31/05/24

.....

Place – Kolkata

Date – 31 May 2024

Pawan Kumar

Chemical Engineering Department

Jadavpur University

Table of Contents

Page No.

Abstract……1

Chapter-I……...2

Introduction……...3

1.1 Disadvantages of floral waste…….....5
1.2 Floral waste utilization……...5
1.3 Hydrogen…….....6
1.4 Photocatalytic hydrogen generation…….....8
1.4.1 Benefits of Hydrogen generation in presence of carbonaceous biomass…….……10
1.5 Literature survey……..11
1.6 Research gap……19
1.7 Selection of Tagetes erecta…….....19
1.8 Role of Carotenoid in Photocatalytic hydrogen generation……20
1.9 Selection of CdS as Semiconductor…….....21
1.10 Objective…….....22

Chapter-II……23

2.1 Material and methods……..…….....24

2.2 Preparation of Tagetes erecta powder……..25

2.3 Synthesis of Cadmium sulfide……...26

2.4 Synthesis of Carotenoid-CdS…….....27

2.5 Synthesis of Tagetes erecta-CdS……28

2.6 Characterization of Samples……..29

2.6.1 Structural Characterization…….....29

2.6.1.1 X-ray Diffraction (XRD)…….....29
2.6.1.2 FTIR Specctroscopy……...30
2.6.1.3 Thermogravimetric analysis-TGA…….....31

2.6.2 Morphological Charcterization……31

2.6.2.1 FE-SEM……31
2.6.2.2 Energy dispersive X-ray spectroscopy (EDS)……....35

2.6.3 Electrochemical characterization……33

2.6.3.1 Transient Photocurrent…….....33
2.7.2 Linear sweep voltammetry (LSV)…….....33
2.7.3 Cyclic voltammetry……..33

2.6.4 Optical characterization…….……...34

2.6.4.1 Ultraviolet-visible Spectroscopy…….…34
2.6.4.2 Tauc Plot……...35
2.6.4.3 Photoluminescence spectroscopy…….....36

2.7 Solar simulator……..37

2.7.1 Bandpass filter…….38

2.8 Photocatalytic Hydrogen generation experimental set-up……39

2.9 Study of hydrogen generation……..…….....43

2.9.1 Performance Study…….....40
2.11.2 Performance Analysis……....40

Chapter-III……..43

Result & Discussion…….....43

3.1 Structural characterization…….....44

3.1.1 X-ray diffraction Analysis……..44
3.1.2 FTIR Analysis……45
3.1.3 Thermogravimetric Analysis……46

3.2 Morphological characterization…….....47

3.2.1 FE-SEM……...48
3.2.2 Energy-Dispersive x-ray spectroscopy analysis……...48

3.3 Optical characterization……..49

3.3.1 UV-Vis study……...49
3.3.2 Tauc Plot……50
3.3.3 Photoluminescence (PL) study……..51

3.4 Photo electrochemical study……...52

3.4.1 Methodology of Glassy electrode coating…….52
3.4.2 Cyclic voltammetry…….53
3.4.3 Linear sweep voltammetry…….55
3.4.4 Photo Current……..56

3.5 Photocatalytic Hydrogen generation: Performance analysis……57

3.5.1 Mechanism and Chemical reaction…….....59
3.5.2 Chemical reactions……..60

3.6 Cost Analysis…….61

3.7 Conclusion…….62

Bibliography……64

Table of Figures

Figure No.	Explanation	Page No.
1.1	Schematic representation of inorganic and organic content of solid waste.	3
1.2	Floral waste disposal behind temples.	4
1.3	Flower waste percentage generated from the function halls (Kg/ Ceremony).	4
1.4	Floral waste percentage from temples of Hyderabad (Kg/Temple/Day).	5
1.5	Utilization of floral waste in various areas.	6
1.6	Generation of fuel.	6
1.7	Represent the hydrogen production according to method involved in it.	8
1.8	General schematic of photocatalytic hydrogen generation.	9
1.9	Tagetes erecta.	19
1.10	Structure formula of Lutein.	20
2.1	Schematics for preparation of Tagetes erecta powder.	25
2.2	Schematic of Cadmium sulfide powder synthesis.	26

2.3	Schematics for preparation of Carotenoid-CdS powder.	**27**
2.4	Schematics of Tagetes erecta-CdS powder synthesis.	**28**
2.5	Bragg's diffraction.	**29**
2.6	Schematic of 'Fourier Transform Infrared' analysis.	**30**
2.7	Thermogravimetric analysis.	**31**
2.8	Schematic diagram of different parts of Field Emission-Scanning Electron Microscopy.	**32**
2.9	Setup of Transient photocurrent, Linear Sweep Voltammetry, and Cyclic Voltammetry.	**33**
2.10	Schematic of 'Ultraviolet-visible Spectroscopy'.	**35**
2.11	Principle of photoluminescence spectroscopy.	**36**
2.12	Working principle of the solar simulator.	**37**
2.13	420 nm Band Pass Filter.	**38**
2.14	Newport LCS-100 solar simulator.	**38**
2.15	Setup of photocatalytic hydrogen generation.	**39**
3.1	X-ray diffraction spectra of CdS-Tagetes erecta, Tagetes erecta, and Cadmium sulfide.	**44**
3.2	Fourier-transform infrared analysis of Cadmium sulfide, Tagetes erecta-CdS, and Tagetes erecta.	**45**
3.3	Thermogravimetric analysis of Cadmium sulfide, Tagetes erecta-CdS, Tagetes erecta.	**46**
3.4	Field emission scanning electron microscopy analysis of Cadmium sulfide (a), and Tagetes erecta-CdS (b).	**47**

3.5	Energy-dispersive x-ray spectroscopy of Cadmium sulfide (a) and Tagetes erecta-CdS (b).	**48**
3.6	Ultraviolet-visible spectroscopy of Cadmium sulfide, Carotenoid, Tagetes erecta-CdS.	**49**
3.7	Tauc Plot for Band gap calculation of Cadmium sulfide, Carotenoid, and Tagetes erecta-CdS.	**50**
3.8	Photoluminescence analysis of CdS, Carotenoid-CdS, and Tagetes erecta-CdS.	**51**
3.9	Setup of electrodes used for photocurrent, Cyclic and Linear sweep voltammetry analysis.	**52**
3.10	Cyclic voltammetry of Cadmium Sulfide with different Source rates.	**53**
3.11	Cyclic voltammetry of Tagetes erecta-CdS with different Source rates.	**54**
3.12	Linear sweep voltammetry of Cadmium sulfide, and Tagetes erecta-CdS.	**55**
3.13	Photocurrent comparison of Cadmium sulfide and Tagetes erecta-CdS.	**56**
3.14	Amount of Hydrogen generated versus irradiation time using Cadmium sulfide, Carotenoid-CdS, and Tagetes erecta-CdS	**57**
3.15	Photocatalytic activity comparison of different photocatalyst.	**58**
3.16	Mechanism of photocatalytic process.	**59**

List of Tables

Figure No.	Explanation	Page No.
1.1	Energy content of different fuels.	7
1.2	Performance of different Biomass Substrates used for Hydrogen Generation.	10
1.3	Literature Survey	11
1.4	Lutein content of various flowers.	21
1.5	Band gaps of different photocatalysts.	22
2.1	Chemicals used for synthesis and characterization.	26
2.2	List of Instrument used for experimental study of hydrogen generation.	26
2.3	Field Emission-Scanning Electron Microscopy parts and their works.	34
3.1	Onset and offset values of Cadmium Sulfide with different source rates.	56
3.2	Onset and offset values of Tagetes erecta-CdS with different source rates.	57
3.3	Millimoles of Hydrogen evolved and Photocatalytic activity of CdS, Carotenoid-CdS, and Tagetes erecta-CdS.	61
3.4	Comparative analysis of Photocatalytic hydrogen production from raw biomass with synthesized photocatalyst.	62
3.5	Cost analysis of Hydrogen generation.	64

Abstract

Enhanced solar hydrogen generation through photocatalytic water splitting utilizing floral waste biomass of yellow colored Tagetes erecta (Marigold) is reported in this thesis. Tagetes erecta is chosen due to the its higher content of organic dye carotenoid. Presence of carbonaceous moiety of biomass acting as a substrate, reduces the thermodynamic barrier of uphill water splitting reaction and increases the rate of hydrogen generation. Organic pigment, carotenoids of Tagetes erecta acting as the photosensitizer, absorbs visible light and transfer electron to the semiconductor photocatalyst CdS.. Experimentally, fine powder of Tagetes erecta is extracted from waste flower and hybridized with the synthesized nano-rods of CdS, by hydrothermal method to form a nanohybrid Tagetes erecta-CdS. Also, for comparison purpose, only carotenoid part extracted from Tagetes erecta floral biomass is hybridized with CdS to synthesize carotenoid-CdS nanohybrid. Structural and morphological (XRD, FTIR, TGA, FE-SEM, EDS), optical (UV-Vis, and PL), and photo-electrochemical (CV, LSV, and Transient photocurrent analysis) characterization of Tagetes-erecta-CdS photocatalytic system are performed and it is tested for hydrogen generation in presence of water, sacrificial agent Na_2S and solar irradiation (full band) using solar simulator of 1 sun intensity. The results show the successful synthesis of photocatalytic material with a larger surface area, lower recombination rate of holes and electrons and better redox reaction. Tagetes erecta–CdS photocatalyst shows high-performance hydrogen generation due to the presence of organic carotenoid and carbonaceous moiety. The Tagetes erecta-CdS photocatalytic system exhibits almost seven times higher hydrogen generation of **~ 35 mmol.g^{-1}.hr^{-1}** compared to pristine CdS **~5 mmol.g^{-1}.hr^{-1}** under full band irradiation. Using a 420 nm band pass filter, **~17%** apparent quantum efficiency (AQY %) is attained. A probable mechanism of enhanced hydrogen generation through water splitting in presence of biomass containing organic pigment, is proposed. The work has significance in context of solar hydrogen generation on a commercial scale and floral waste management.

Keywords: Tagetes erecta,) Carbonaceous Biomass, Carotenoid, Photocatalytic hydrogen generation, Water splitting

****

Chapter-I

Introduction
&
Literature Review

Introduction:

Population growth, global urbanization and industrialization are the major causes for production of waste materials[1]. Waste management has direct impact on the financial development of the nation [2]. Utilization of solid waste as the raw material to produce valuable product allows one to recycle it back to the industries and fulfil the mission of the country 'Waste to Wealth' Waste management can help to improve lifestyle and build a healthy environment[3].

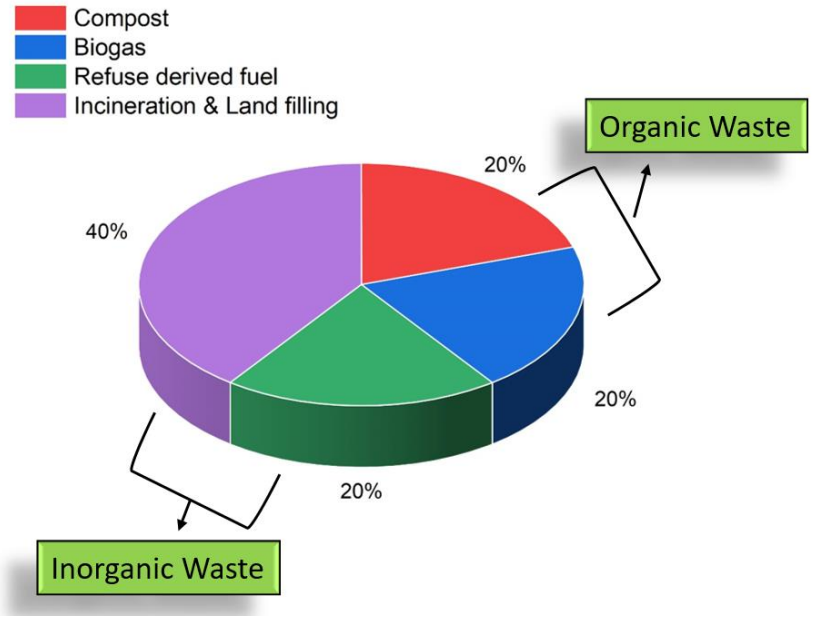


Fig 1.1: Schematic representation of inorganic and organic content of solid waste[4].

Both the inorganic and organic solid waste (Fig 1.1) materials emanate from industrial, commercial, and residential places, institutions, hospitals, hotels, vegetable markets etc. These waste materials are the route of pollution and threat for society, if they are not handled properly.[4]

Waste flowers are found from different residential, cultural and religious places. These floral wastes can be collected in bulk form from various religious places such as temple, monastery, dargah etc. On daily basis, lot of the flowers and floral plants after being used, get wasted and hence become garbage. This floral waste gets accumulated at the religious sites (refer to Fig1.2)[5].



Fig 1.2: Floral waste disposal behind temples[6].

In India, among various flowers the red and yellow coloured Marigolds are found as the main components of flower waste (Figs. 1.3 and 1.4).

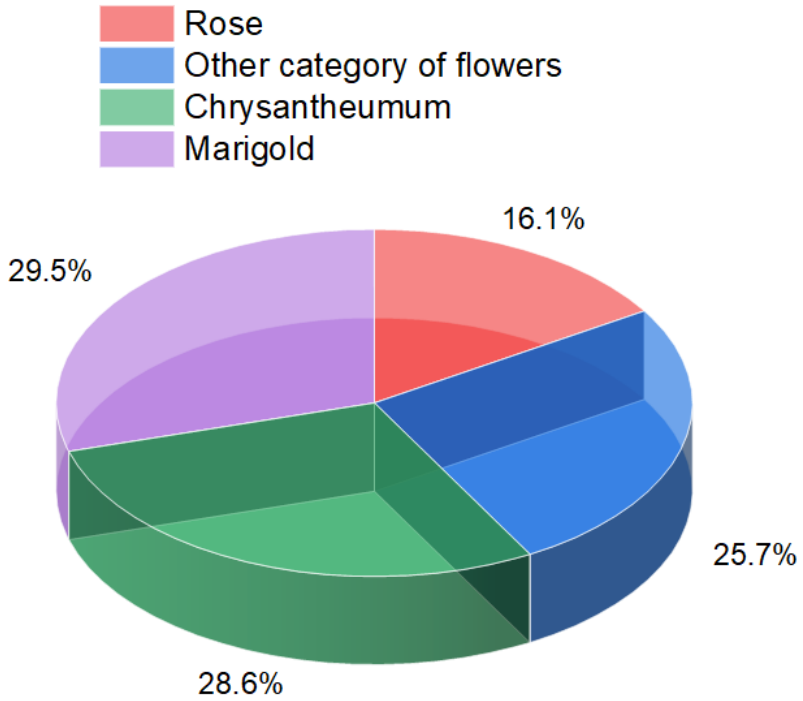


Fig 1.3: Flower waste percentage generated from the function halls (Kg/ Ceremony).[7]

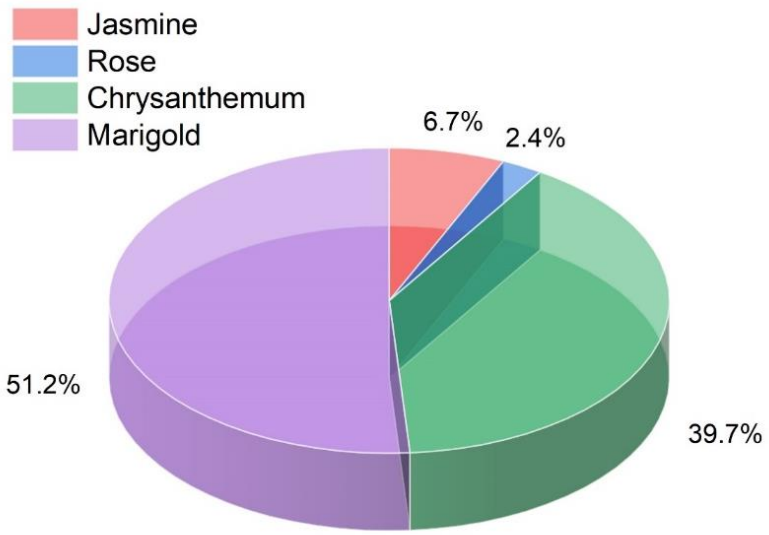


Fig 1.4: Floral waste percentage from temples of Hyderabad (Kg/Temple/Day)[7].

1.1 Disadvantages of floral waste:

- Floral waste dumped into water reservoir raises the biological oxygen demand (BOD) and hence causes undesired contaminants.
- Municipal solid waste together with flower waste raise the level of leachate that shows adverse effect on water bodies.
- The floral waste causes insects to attract as well as forms breeding ground of mosquitoes thereby spreads contagious disease specified areas.
- Bacterial action breaks down organic wastes in a series of phases, producing methane and carbon dioxide. Methane has high potential to cause global warming (at least 72 times more potent than CO_2[8].

1.2 Floral waste utilization:

The floral waste can be utilized as a resource rather than being discarded in landfills, which causes a slew of difficult-to-manage environmental concern. All floral waste of the community waste like weddings, religious places, floral market waste, residential floral waste, etc. can be onverted into various products namely bioethanol, bio-gas, vermi-compost, essence etc. (Fig 1.5).

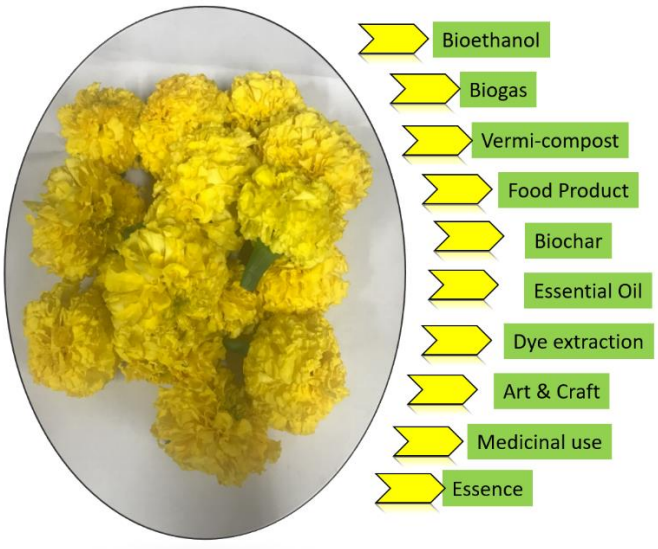


Fig 1.5: Utilization of floral waste in various areas[9].

1.3 Hydrogen:

Fossil fuels has been the major source of energy production at present that produces different types of harmful pollutants. The atmospheric pollution happens due to greenhouse gases like Carbon oxides, Nitrogen oxides, and Methane. The energy content and carbon percentage of the different types are shown in Table 1.1 Hydrogen is the most suitable replacement of fossil fuels (refer to Fig 1.6) due to its high energy content and zero emission of greenhouse gases.

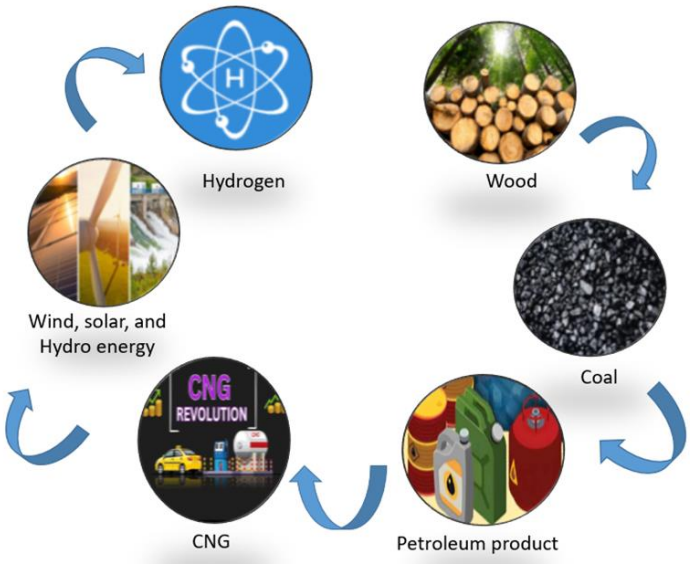


Fig 1.6**:** Generation of fuel.

Fuel	Lower Heating Value (MJ/Kg)	Energy/unit mass (MJ/Kg)	Carbon Percentage (%)	Reference
Softwood (average)	16-20	20.3	52.4	[10]
Coal (anthracite)	33.3	15-19	50	[11]
Petrol (naptha)	44.9	40-43	86	
Natural Gas	38.1	33-50	46	
Hydrogen	**120.1**	**120**	**0**	

Table 1.1: Energy content of different fuels.

Hydrogen is available in nature in the form of hydrocarbons and water. Hydrogen is an effective energy carrier and clean fuel. It can be utilized across numerous industries because of its broad range of use. Hydrogen is utilized as a fuel in fuel cell to generate electricity with water as the by-product[12]. Hydrogen also has some drawbacks such as low density, safety related issues; compared to fossil fuel it has low ignition energy. Hydrogen is a potentially good fuel against climate change. It is proposed that by 2050, most of the country will run on hydrogen and will attain the goal of zero carbon emissions[13].

Industries are practicing hydrogen generation from various methods most of them are based on reforming fossil fuels. At present, 95% of hydrogen is getting produced from fossil fuels like coal, petroleum, and natural gas. These fuels are not a practical source of hydrogen gas because they are non-renewable sources and also carbon dioxide will be produced from them during the hydrogen generation process, which will cause global warming[13]. Fig 1.7 depicts different category of hydrogen depending on method of synthesis and sources. The advantageous strategy of green hydrogen generation is the utilization of renewable feedstock, which reduces carbon emissions.

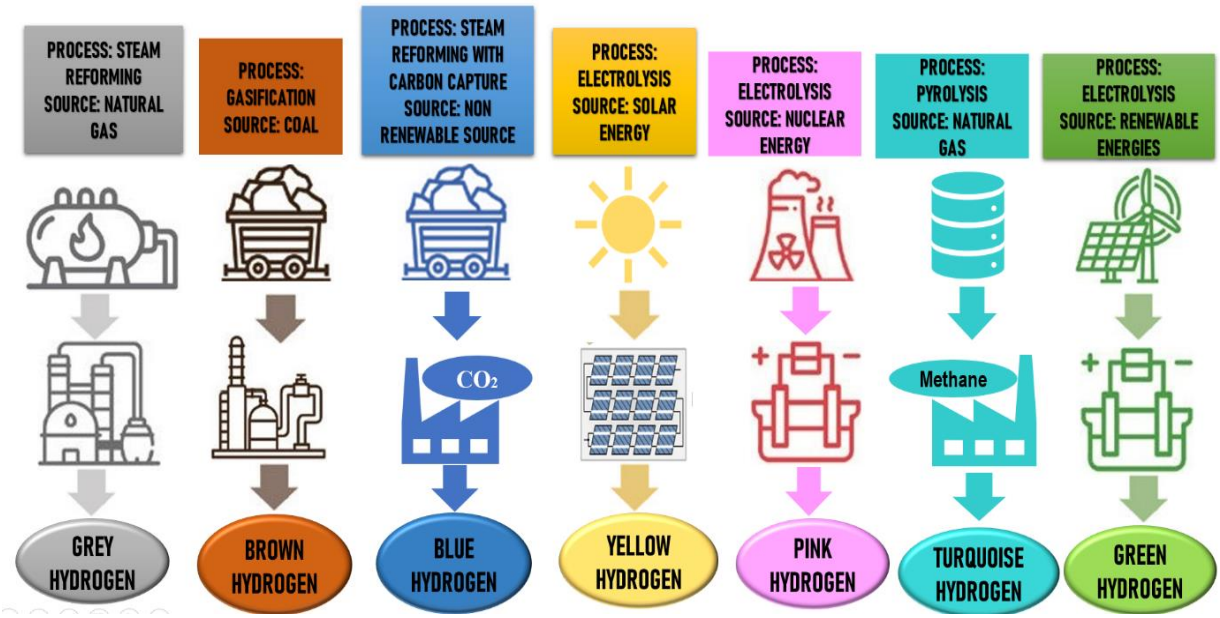


Fig 1.7: Different category of Hydrogen depending on production method and source.

In this work, the focus is mainly on the production of green hydrogen. A few challenges are needed to overcome for enhanced green hydrogen production such as the choice of proper feedstock and a proper photocatalyst. However, the research is ongoing continuously to overcome the bottlenecks and generate a high quantity of hydrogen[13]The photocatalytic process was first developed by Fujishima and Honda in the 1970s using titanium oxide as a catalyst and platinum as a counter electrode for hydrogen generation; after that various scientists have shown their interest in hydrogen generation via photocatalytic processes[14].

1.4 Photocatalytic hydrogen generation via water splitting:

Photocatalytic hydrogen generation is a process which uses sun light to produce hydrogen from water. This method simply includes a semiconductor photocatalyst that absorbs light to start the chemical reaction for hydrogen generation.

Photocatalytic water splitting, a thermodynamically uphill reaction convert water to hydrogen and oxygen in presence of solar irradiation and semi-conductor photocatalyst [15]. Fig 1.8 shows the mechanism of water splitting (without biomass). The mechanism involves several steps for hydrogen generation such as:

Absorption of photons and generation of electron-hole pair when photons are absorbed by a semiconductor, it generates an electron-hole pair which is involved in redox reaction for hydrogen generation.

Oxidation reaction: Formation of oxygen and hydrogen ions (H^+)

Reduction reaction: Formation of hydrogen

Reactions involved in water splitting:

Reduction: $2H^+ + 2e^- \rightarrow H_2$	$E^0 = 0$ V		(1.1)
Oxidation: $H_2O \rightarrow 2H^+ + ½\ O_2 + 2e^-$	$E^0 = +1.23$ V		(1.2)
Overall reaction: $H_2O \rightarrow H_2 + 1/2\ O_2$	[$\Delta G_0 = 237.1$ kJ mol^{-1}]	$E^0 = -1.23$ V	(1.3)

bottlenecks viz. thermodynamic barrier, photo corrosion,, light conversion efficiency, low quantum yield and high recombination; these lowers the quantum efficiency and restricts the commercialisation of the process[17].

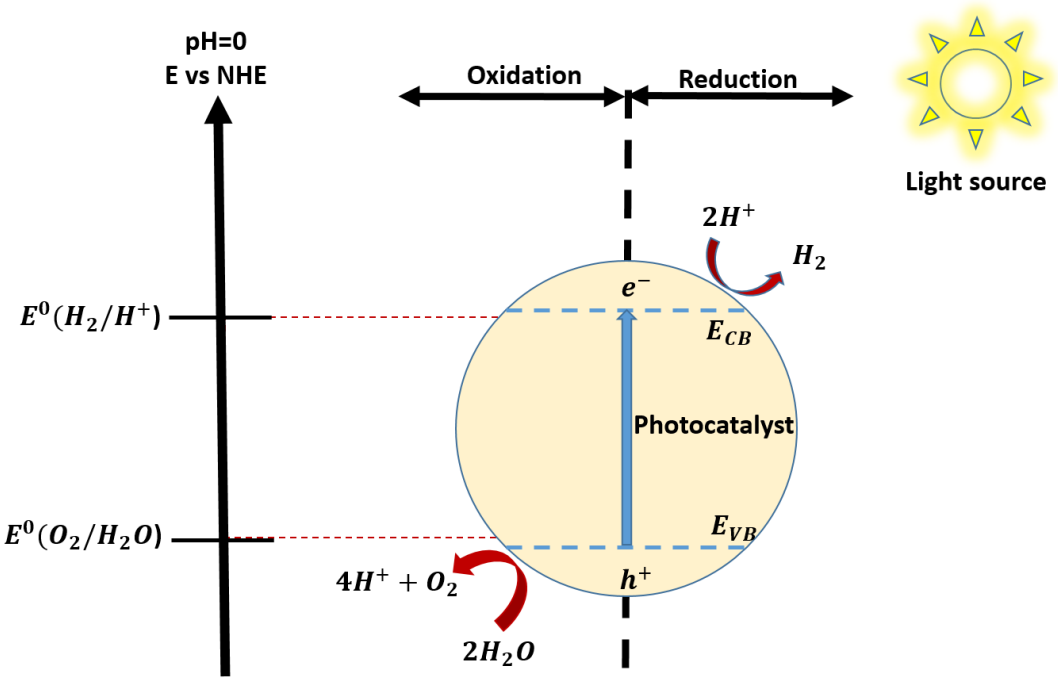


Fig 1.8: General schematic of photocatalytic hydrogen generation.

1.4.1 Benefits of Hydrogen generation in presence of carbonaceous biomass:

The inclusion of carbonaceous biomass as a substrate along with water and sunlight (biomass reforming) lowers the thermodynamic barrier of conventional water splitting. The photocatalytic reforming of oxygenates can be viewed as the sum of the oxidation of carbonaceous biomass and water splitting.

Oxidation of Biomass

$C_xH_yO_z + \left(x + \frac{y}{4} - \frac{z}{2}\right) O_2 \rightarrow \frac{y}{2} H_2O + xCO_2 \qquad (\Delta G_0 < 0\ ;\ \Delta H_0 < 0)$ (1.4)

Water Splitting

$H_2O \leftrightarrow H_2 + ½\ O_2 \qquad [\Delta G0 = 237.1\ kJ\ mol^{-1}] \qquad E^0 = -1.23\ V$ (1.5)

Overall reaction:

$CxHyOz + (2x - z)\ H2O \rightarrow (2x + y/2 - z)\ H2 + x\ CO2$ (1.6)

While water splitting (equation 1.5) is an energy consuming process, the oxidation of organic substances (biomass) (equation 1.4) is exergonic and exothermic; the combination of both reactions (equation 1.6) may result in slightly up-hill reforming process [18]. A significantly higher rate of hydrogen production can be achieved by this process from a variety of feedstock's, which could be chosen from waste material. Small amount of other gas (CO_2) is also produced through this process of water splitting in presence of carbonaceous biomass; the sacrificial agent is used to control the production of other gas. Examples of different types of biomass (reported in literature) used as substrate for low-cost hydrogen generation are tabulated in Table 1.2:

Substrate Name	**Photo-Catalyst Name**	**Activity (mmol (H_2).g^{-1}.hr^{-1})**	**Reference**
Grass	Co/CdS/CdO_x	1.0	[18]
Sawdust	Co/CdS/CdO_x	0.75	
Wooden branch	Co/CdS/CdO_x	5.31	
Rice husk	0.5 % Pt/TiO_2	0.095	

Table 1.2: Performance of different Biomass Substrates used for Hydrogen Generation.

The factors those affect hydrogen generation from biomass are the type of biomass feedstock, type of semiconductor photo-catalyst, and reaction temperature, pressure[19].

1.5 Literature survey:

Table 1.3

SI. No.	Year	Author	Vol. & Page no.	Title	Journal	Description
1	2024	Rika Taslim, et al.	285 & 119566	Synthesis of highly self-N-O-dual doped unique carbon blooming flower-like nanofiber derived novel snake-plant waste for ultrahigh energy of solid-state-supercapacitor	Chemical Engineering Science	• In this literature the author tried to develop a bio-organic material of nitrogen and oxygen self-dual doping with carbon composite nanofiber utilizing green snake plant. • The author has developed a supercapacitor mainly a basic component of electrode composition. • The cell using this method has shown a holding capacity and Columbia efficiency of 76.94% and 95.27% with output energy of 27.37 $Wh.kg^{-1}$ and 0.72 Ω resistance.
2	2022	Sofia Semitsoglou-Tsiapou, et al.	286, Part 3 & 131697	Photochemical (UV–vis/H_2O_2) degradation of carotenoids: Kinetics and molecular end products	Chemosphere	• The aim of this literature to study and determine the relative kinetics reaction and product degradation of specified hydrated carotenoids under UV-Vis/H_2O_2 experimental conditions. • In this literature, a comparison has been made between β-Carotene, fuco-xanthin, and meso-zeaxanthin, which of them is important of the ocean food webs. • The binary solvent of (THF: H_2O) of 1:9 has

						been used for oxidation experiments due to carotenoids do not dissolve in water.
3	2024	Ritu Jangra , et al.	75 & 109728	$ZnCl_2$-assisted conversion of nitrogen-containing biomass carbon from marigold flower: Toward highly porous activated nitrogen-doped carbon for low ESR and enhanced energy density supercapacitors	Journal of Energy Storage	• Biomass of marigold flower and $ZnCl_2$ composition has been done in the ratio of 1:1, 1:3, and 1:5. • In this reported literature the author tried to develop various kinds of carbon structures for EDLC to overcome the energy density problem. • The author has used a process to dope the nitrogen on the activated carbon for a large surface area.
4	2021	Icuk Dian Likasari, et al.	780 & 138914	NiO nanoparticles synthesized by using Tagetes erecta L leaf extract and their activities for photocatalysis, electrochemical sensing, and antibacterial features	Chemical Physics Letters	• From the previous few reported papers, the author synthesized material NiO nanoparticles together with extracted Tagetes erecta leaf as bio-reductor. • The two methods that have been used for the development of synthesized material are reflux and microwave irradiation methods. • From the analysis, it has been reported that the synthesized nanoparticle is effective against Gram-positive and Gram-negative bacteria.
5	2021	Subhadeep Ghosh, et al.	279 & 130515	Facile synthesis of carbon dots from Tagetes erecta as a precursor for determination of chlorpyrifos via fluorescence turn-off and	Chemosphere	• In this literature, a synthesis of Carbon dots has been done using Tagetes erecta as precursor using the hydrothermal method.

				quinalphos via fluorescence turn-on mechanisms		• The prepared carbon dots have shown excellent detection properties of chlorpyrifos and quinalphos pesticides using turn-on and turn-off fluorescence mechanisms.
6	2021	Gopal Krishna, et al.	46 & 38416-38424	Excellent supercapacitive performance of graphene quantum dots derived from a bio-waste marigold flower (Tagetes erecta)	Hydrogen Energy	• In this literature, Graphene quantum dots of Tagetes erecta flower have been done through hydro-thermal carbonization to use in supercapacitor as an electrode material. • This report has put an effort into the energy storage application of supercapacitors.
7	2021	Hajer Naif Alotaibi, et al.	66 & 162-168	Influence of lutein content of marigold flowers on functional properties of baked pan bread	Annals of Agricultural Sciences	• In this literature, Lutein content of Tagetes erecta biomass has been extracted to ustilize as a gradient to enhance the colour and to increase the anti-oxidant properties of bread. • The method for Tagetes erecta conversion to biomass can be oven, free, and vaccum drying.
8	2017	Mahdi Karimi-Nazarabad. et al.	160 & 484-493	Highly efficient photocatalytic and photoelectrocatalytic activity of solar light driven WO_3/g-C_3N_4 nanocomposite	Solar Energy Materials & Solar Cells	• In this literature nanocomposite of WO_3/g-C_3N_4 synthesized in the ratio of (1:1, 1:1, 3:1). • Photocatalytic activity of synthesized material has been calculated using a Reactive black 5, and azo dye photodegradation under solar irradiation. The synthesized material has a better band gap which makes it a better nanocomposite for photoelectrochemistry and photocatalysis.

9	2021	Thibaut Lepage, et al.	144 & 105920	Biomass-to-hydrogen: A review of main routes production, processes evaluation and techno-economical assessment	Biomass and bioenergy	• In this literature, biomass to hydrogen conversion has been reviewed. • The method which is majorly used to generate hydrogen from biomass involves biological, thermochemical, and electrochemical. • All of these have their pros & cons. This literature has reported biomass to hydrogen generation is the most promising way for hydrogen generation and the contribution to society, but some challenges must be overcome like optimization to large scale for industrial production.
10	2011	Huizhi Zhou, et al.	219 & 188-194	Dye-sensitized solar cells using 20 natural dyes as sensitizers	Journal of Photochemistry and Photobiology A: Chemistry	• In this report, the author has extracted 20 types of natural dyes from fruits, flowers, beverages, leaves, and traditional Chinese medicines. • The dyes used in Dye-sensitized solar cells to evaluate their photoelectrochemical performance in short-circuit photocurrent density, open circuit voltage, and photo-to-electric conversion efficiency. • The literature has reported that mangosteen pericarp extracted dye has high open circuit voltage and photo-to-electric efficiency of about 1.17% with no purification.

11	2017	Siti Nur Hidayah Jaafar, et al.	78 & 698-709	Natural dyes as TIO_2 sensitizers with membranes for photoelectrochemical water splitting: An overview	Renewable and Sustainable Energy Reviews	• The literature has reported that TiO_2 is efficient material for photocatalytic method but due large band gap it have limited capacity to store visible light and electron-hole recombination also effect the efficiency of it. • To overcome it a natural stand has a suitable candidate due its fast electron transferring ability. • There are several method has been reported in this review paper for extraction of dye in which some of them are cost effective process. • Using the synthesized nanocomposite material of TiO_2 using dye will overcome limited ability and provide higher efficiency.
12	2021	V.K.M. Katta, et al.	45 & 794-798	Green synthesis of silver nanoparticles using Tagetes erecta plant and investigation of their structural, optical, chemical and morphological properties	Materials Today: Proceedings	• This literature reports the Greensynthesis of silver nanoparticles using Tagetes erecta plant. • The addition of biomass acts as a reducing agent and makes it less toxic. • This study shows the silver nanoparticles' potential as a catalyst for photodegradation.
13	2019	Yi-Hsuan Chiu, et al.	7 & 080901	Photoelectrochemical cells for solar hydrogen production: Challenges and opportunities	APL materials	• This article is based on photoelectrochemical water splitting challenges and opportunities for solar hydrogen generation. • In situ and operando spectroscopic techniques are used to improve the understanding of

						photoelectrochemical processes. • To utilization of more of solar spectrum development of NIR-responsive photoelectrode has been used.
14	2021	Yanxiang Liu, et al.	27 & 479-489	Semi-Synthetic Chlorophyll-Carotenoid Dyad for Dye-Sensitized Photocatalytic Hydrogen Evolution	Advanced Materials Interfaces	• In this literature, a novel approach of the synthesis of chlorin-carotenoid dyad (Dyad-COOH) for photocatalytic hydrogen generation. • The synthesized nanoparticle consists of a carotenoid moiety that is used for light-harvesting and chlorin for photosensitivity together with COOH. • The report shows that chlorin-carotenoid dyads are low-cost photosensitizers for PHE to develop better catalysts.
15	2015	Ana Flavia Burlec, et al.	12 & 887	Eco-Friendly Synthesis and Comparative In Vitro Biological Evaluation of Silver Nanoparticles Using Tagetes erecta Flower Extracts	Applied sciences	• This literature focuses green synthesis route to synthesize silver nanoparticle using an extract of Tagetes erecta. • Ethanolic and aqueous extract of Tagetes erecta has been utilized to synthesize the silver nanoparticle. • This synthesized nanoparticle has shown desirable properties such as spherical morphology and biological activities (antioxidant and antimicrobial) properties.
16	2009	Akihiko Kudo	38 & 253-278	Heterogeneous photocatalyst materials for water splitting	Chem Soc Rev	• The literature review has shown various photocatalyst which have been recently developed, that are expanding the

						efficiency of photocatalytic water splitting process. • The modification of photocatalyst has been going on to achieve up to 5% solar energy conversion. • This review has reported that advancement in photocatalysis will contribute major role in global energy demand and environmental issues.
17	2016	Xiaohu Zhang, et al.	4 & 2365	Recent advances in dye-sensitized semiconductor systems for photocatalytic hydrogen production	Journal of Material Chemistry A	• This review paper mainly focused on the fundamentals and advancement in dye-synthesized photocatalysts that will work in visible and nearby IR ranges for hydrogen production. • Several dye-synthesized photocatalysts have been discussed briefly.
18	2022	Ajay Singh, et al.	3 & 1341-1358	Application of carotenoids in sustainable energy and green electronics	Material Advances	• This literature review is focused on carotenoid application in optoelectronic and electronic devices with its advantages. • Carotenoid semiconducting nature, solution processability, and natural presence make it a suitable candidate for many applications. • This paper has reported that modifying TiO_2 with carotenoid has been used to harness solar irradiation for hydrogen generation. • Using carotenoids, several devices like transistors, rectifiers,

						sensors, and LEDs have been made. • Up to now only a few carotenoids have been explored, but there various types of carotenoids available which is unexplored.
19	2021	Praveen Kumar Gopi, et al.	45 & 3022-3033	Cadmium sulfide quantum dots anchored on reduced graphene oxide for the electrochemical detection of metronidazole	NJC	• This paper has reported the synthesis and application of composite material of CdS quantum dots and rGO nanosheets for metronidazole electrochemical detection. • This metal organic-based synthesis of CdS quantum dots with rGO nanosheet has been done using simple sonication. • The nanocomposite of CdS quantum dots with rGO has been coated on a glassy electrode for detection of MTZ.
20	2023	Sayantanu Mandal, et al.	51, Part B & 1167-1185	Organic alginate encapsulated rGO-CdS millisphere for remarkable photocatalytic solar hydrogen production.	Hydrogen Energy	• This literature has reported a remarkable hydrogen generation (79.68 $mmol.g^{-1}.hr^{-1}$) • The synthesis process involves the modified Hummer's method for graphene oxide and CdS synthesis using Cadmium acetate dehydrate and thiourea. After that hydrothermal process is used for rGO-CdS synthesis, and then encapsulation of the synthesis material is done by using food-grade sodium alginate. • The paper has confirmed the reduction in toxicity level using cell viability testing.

						• Due to encapsulation photo corrosion will be less, and entrapped water will do reaction rapidly. • A single bead itself acts as a continuous reactor.

1.6 Research gap:

- Floral biomass containing organic dye has not been explored for enhanced solar hydrogen generation.

The goal of the present work is enhanced hydrogen generation using floral biomass of Tagetes erecta containing high content of organic pigment Carotenoid that acts as photo-sensitizer.

1.7 Selection of Tagetes erecta

Tagetes erecta is also known as Aztec marigold, Mexican marigold, cempasúchil or cempaxochitl. It is a flowering plant species; it appears under the genus of Tagetes that are native to Mexico and Guatemala. Thus, often it is known as Mexican marigold and African marigold (Table 1.4).

Botanical Study:

Kingdom: Plantae

Order: Asterales

Family: Asteraceae

Genus: Tagetes

Species: Erecta



Fig 1.9: Tagetes erecta.

- **Uses of Tagetes species:**

The yellow colored Tagetes erecta is composed two parts organic dye carotenoid, and carbonaceous part[20]. Among different colored flowers, Tagetes erecta is chosen due to its high carotenoids content (Table:1.4); it contains around 90% Lutein and 5% zeaznthin Lutein is a xanthophyll or oxycarotenoid, comprising of 2 cyclic hydrocarbon rings (one alpha-ionone ring and one beta) and the basic C-40 isoprenoid structure (Fig 1.10).

It is a key component and primary pigment of Tagetes erecta. The carbonaceous biomass part of Tagetes erecta along with water, as feedstock for hydrogen generation, contain huge amounts of energy in the form of hydrogen bonds [21].

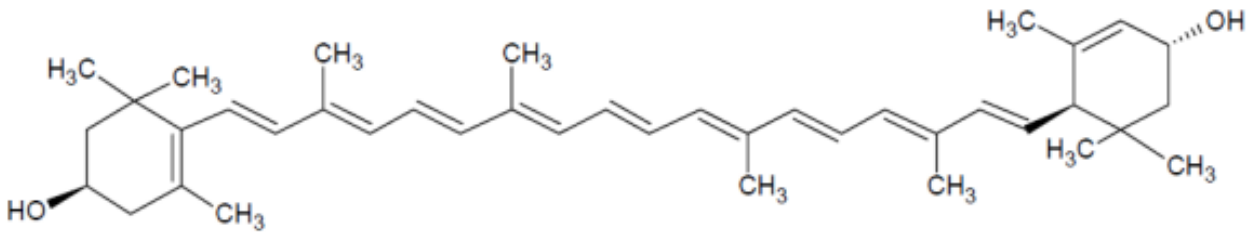


Fig 1.10: Structure formula of Lutein[22].

1.8 Role of Carotenoid in Photocatalytic hydrogen generation:

Carotenoid works as a photo-sensitizer that actively traps the photons of 400-600 nm and rapidly transfers the electrons to form their cations (Car*). Photon excited electrons are transported from dye to CB of inorganic semiconductor and these electrons are used to generate hydrogen. In presence of photosensitizer dye carotenoid (visible light absorber), charge separation is simpler than in a semiconductor photocatalyst because charges can be separated from the dye to the inorganic semiconductor. It has been previously reported that a concentration of carotenoid lower than 30 µM with TiO_2 increased the production of oxygen radicals in solar irradiation. Thus, carotenoid radicals together with photocatalyst promote oxidation of biomass and enhance hydrogen generation through water splitting[21].

Scientific Name	Common Name	Part Flower	Colour	Total Carotenoids (µg/g)	Ref.
Dendranthema gradiflorum (Ramat.) Kitam.	Chrysanthemum	Flowers (different cultivars)	Purple, White, Green, Red, Yellow	19–346	[23]
Tagetes patula L.	French marigold	Petals	Yellow and orange	270–2020	[24]
Helianthus annuus L.	Sunflower	Petals	Yellow and orange	144–1600	[24]
Chrysanthemum morifolium	Chrysanthemum	Petals	Yellow and orange	122–343	[25]
Tagetes erecta	**Mexican marigold African Marigold**	**Petals**	**Yellow and orange**	**48–2130**	[25]
Cucurbita maxima Duchesne	Squash flower	Flowers	Yellow	12–188	[26]
Petunia × hybrida Vilm.	Garden petunias	Flowers	Solid colour or bicolour (Red, rose, pink, blue, burgundy, white, yellow)	0.32–96.8	[27]

Table 1.4: Lutein content of various flowers.

1.9 Selection of CdS as Semiconductor

Cadmium sulfide is a semiconductor of group II-VI with a bandgap of 2.45 eV[28] [29]. Cadmium sulfide has various excellent chemical and physical properties that have multiple uses in various fields which also include photochemical catalysis. Cadmium sulfide can be formed by various methods of thermal decomposition, solvothermal/hydrothermal methods, etc.[30][31] Cadmium sulfide shows sustained photocatalytic reactions because of high

photostability under long-time light exposure. Its low cost and availability in nature make it cost-effective[32].

The conduction band of cadmium sulfide is lower than other common semiconductors such as $SrTiO_3$, ZnO, and TiO_2. CdS properties can be fine-tuned by multiple methods such are size control, doping and surface modification, for enhanced performance in the application of hydrogen generation. Loading of co-catalysts like nickel (Ni), platinum (Pt), or cobalt (Co) can enhance the efficiency of photocatalytic hydrogen generation rather than bare CdS[33].

Semiconductor	Band Gap Structure (pH = 7)			Reference
	Cb	Vb	Eg/eV	
$SrTiO_3$	0.7	2.5	3.2	[29]
ZnO	0.31	2.89	3.19	[34]
TiO2	0.50	2.70	3.22	[35]
ZnS	1.04	2.56	3.6	[36]
CdS	**0.90**	**1.50**	**2.45**	[28]

Table 1.5: Band gaps of different photocatalysts.

1.10 Objectives:

The specific objectives of this work are as follows:

- Collection of waste Tagetes erecta and synthesis of Tagetes erecta powder
- Synthesis of Tagetes erecta-CdS nano-hybrid and Carotenoid-CdS nanohybrid.
- Structural, morphological, optical and photoelectrochemical characterization of the synthesized nano-hybrids.
- Study of performance of synthesized Tagetes erecta-CdS and Carotenoid-CdS nanohybrid in hydrogen generation through photocatalytic water splitting
- Evaluation of photocatalytic activity and apparent quantum efficiency
- Prediction of proposed mechanism of photocatalytic water splitting in presence of biomass and carotenoid.

Chapter-II

Experimental Section

2.1 Materials and methods:

Table 2.1 Chemicals used for synthesis and characterization:

Chemical reagents		
Chemicals	**Chemical Formula**	**Brand**
Cadmium Acetate dihydrate	$Cd(O_2CCH_3)_2(H_2O)_2$	Sigma-Aldrich
Thiourea	NH_2CSNH_2	Sigma-Aldrich
Ethanol	C_2H_5OH	Changshu Song Sheng Fine Chemical
Acetone	CH_3COCH_3	Merck
Deionized water	H_2O	Millipore (18.2 mΩ)
Sodium Sulfide	Na_2S	Rankem
Nafion	$C_9HF_{17}O_5S$	Sigma-Aldrich
Isopropyl alcohol	C_3H_8O	Sigma-Aldrich
De-ionized water	H_2O	Millipore (18.2 mΩ)

Table 2.2 List of Instrument used for experimental study of hydrogen generation:

Equipment and Instrument	
Instrument	**Brand**
Vacuum Pump	Rivotek
Laboratory balance	Sartorius
Magnetic Stirrer	Tarsons Products Limited
Hot Air Vacuum oven	----------
Centrifuge	Eppendorf centrifuge 5430 R
Teflon Hydrothermal Container	----------
Muffle Furnace	S. C. Dey & Co.
Power Meter	R173
Solar simulator	Newport

2.2 Preparation of Tagetes erecta powder

The Tagetes erecta waste flowers are collected from religious places, ceremonies, and household waste nearby Jadavpur University, and stored at (≤ 4 ^{0}C) for 12 hrs to keep the Tagetes erecta bacteria-free and fresh. The Tagetes erecta flower petals are removed from flower and washed multiple times with deionized water (18.2 mΩ) for removal of contamination from the petals and then a vacuum pump (300 mm Hg pressure) is used to remove the extra water. The washed floral waste is dried in an electric hot air vacuum oven in dark condition for 8 hrs at 60 ^{0}C for complete removal of moisture and further grounded in a mortar pestle to convert into yellow powder. The yellow powder is then screened through the 100-mesh filter for the removal of large particles. After screening fine particles are stored in a vacuum-sealed container and stored in a desiccator to prevent contamination.

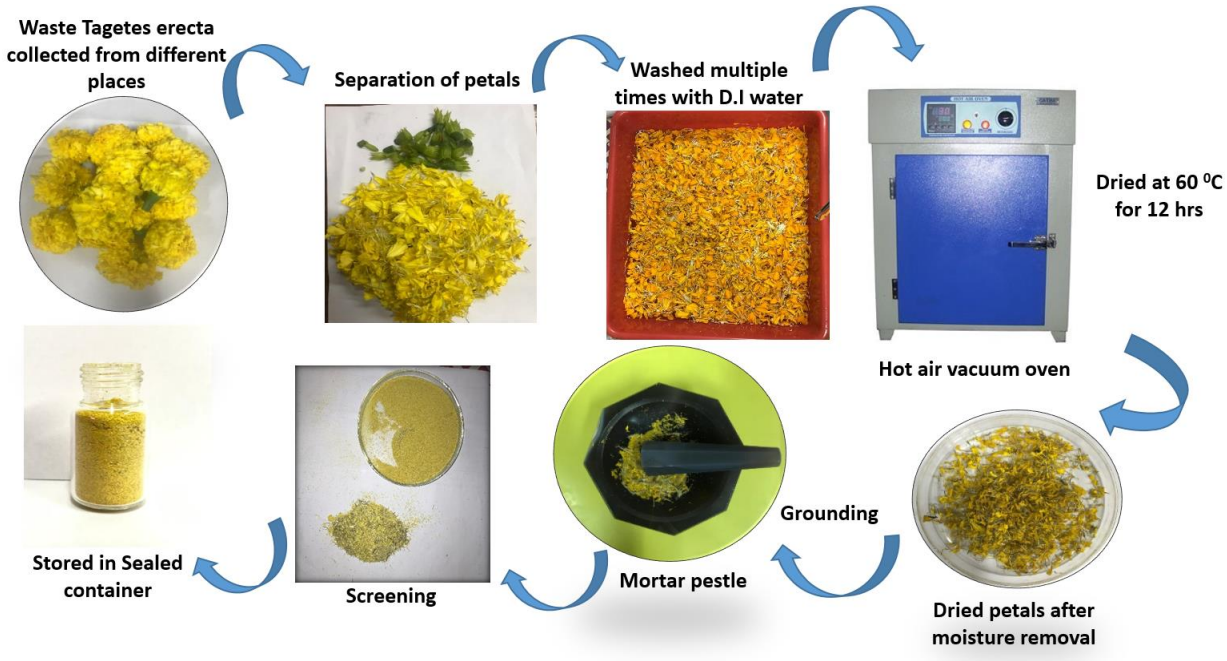


Fig 2.1: Schematics for preparation of Tagetes erecta powder.

2.3 Synthesis of Cadmium sulfide (CdS):

Cadmium acetate (5.56 g) and Thiourea (3.806 g) individually is mixed with 50ml of deionized water (18.2 mΩ) in separated beakers with a vigorous stirring for 1 hour at a speed of 800rpm. After 1 hour, two solutions are mixed and stirred for 10 hrs/ 600 rpm at 80° C. Following 10 hours, the colour of the combination changes from tangerine to yellow. This is an indication that Cadmium sulfide has been synthesized. After that the solution is collected in a petri dish and dried for 2 hours at 80° C in a hot air vacuum oven. The Cadmium sulfide solution is then recovered as fine powder and kept in a desiccator.

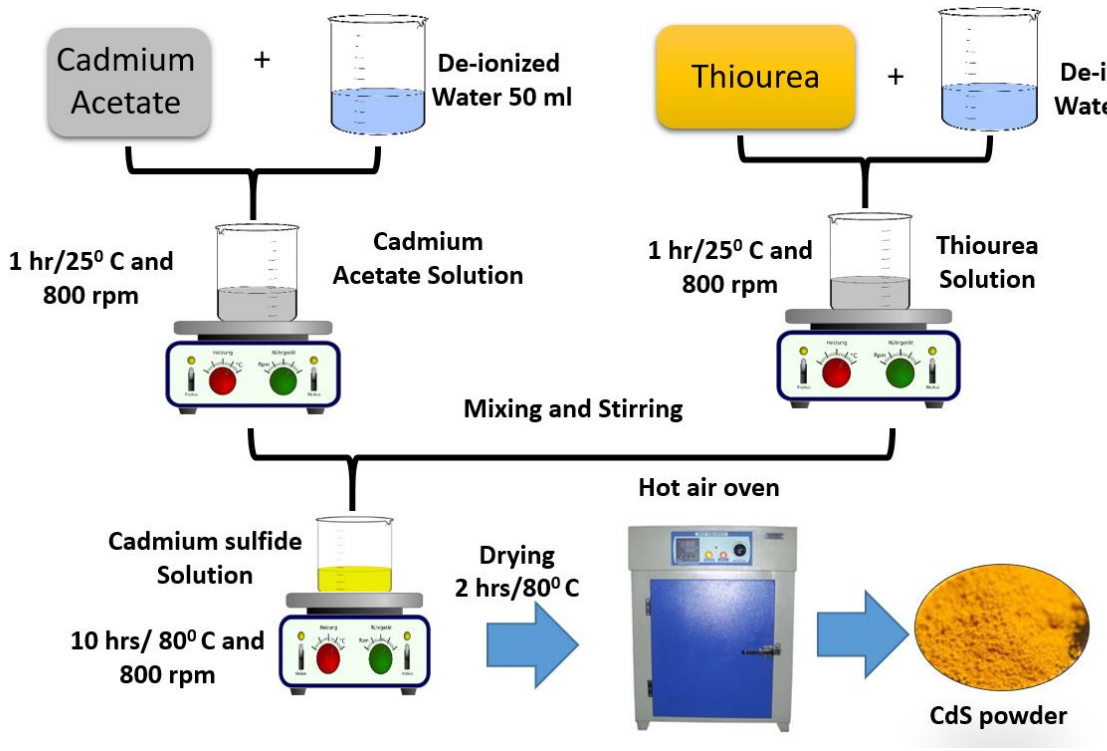


Fig 2.2: Schematic of Cadmium sulfide powder synthesis.

2.4 Synthesis of Carotenoid-CdS:

The extracted Tagetes erecta fine powder is dissolved in acetone and stirred for 4 hours at 600 rpm at room temperature in a dark environment. The mixing is further carried in a vortex for the next 0.25 hours and then the solution is centrifuged (at 7000 rpm) for the next 0.5 hours for carotenoid extraction from the residue. The extraction is repeated until the residue became pale and the accumulated supernatants are stored in a vacuumed chamber to prevent contamination. The carotenoid is mixed with 0.2(M) sodium hydroxide solution and continuously stirred in dark for 2 hrs at 600 rpm at room temperature. Similarly, CdS is dispersed homogeneously in sodium hydroxide solution continuously stirred in a dark for 1 hrs at 600 rpm and 60^0 C. Then the CdS solution and Carotenoid solution are homogeneously stirred for 4 hrs at 60^0 C and 600 rpm. The mixture is kept in a 50-ml Teflon chamber and put in the autoclave at 180^0 C for 18 hours at a rate of 40^0 C. The carotenoid-CdS solution is then separated by centrifugation at 5000 rpm for 5 minutes and subsequently dried at 70 ^oC for 8 hours in an electric air oven in dark conditions.

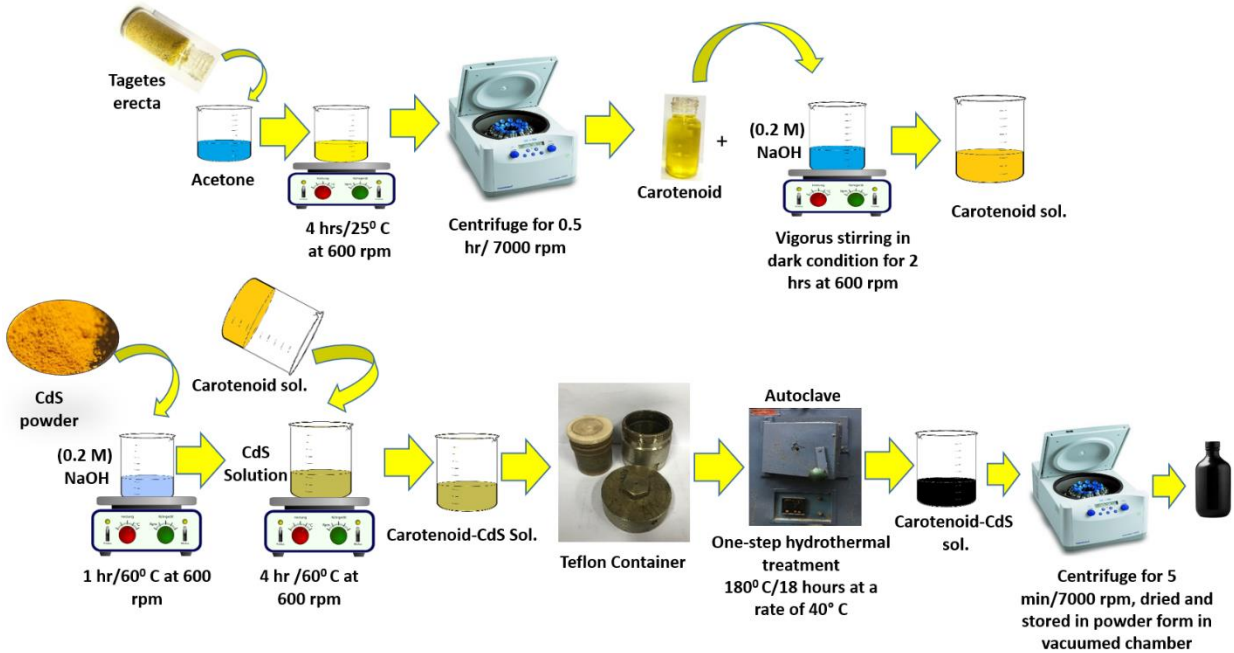


Fig 2.3: Schematics for preparation of Carotenoid-CdS powder.

2.5 Synthesis of Tagetes erecta-CdS:

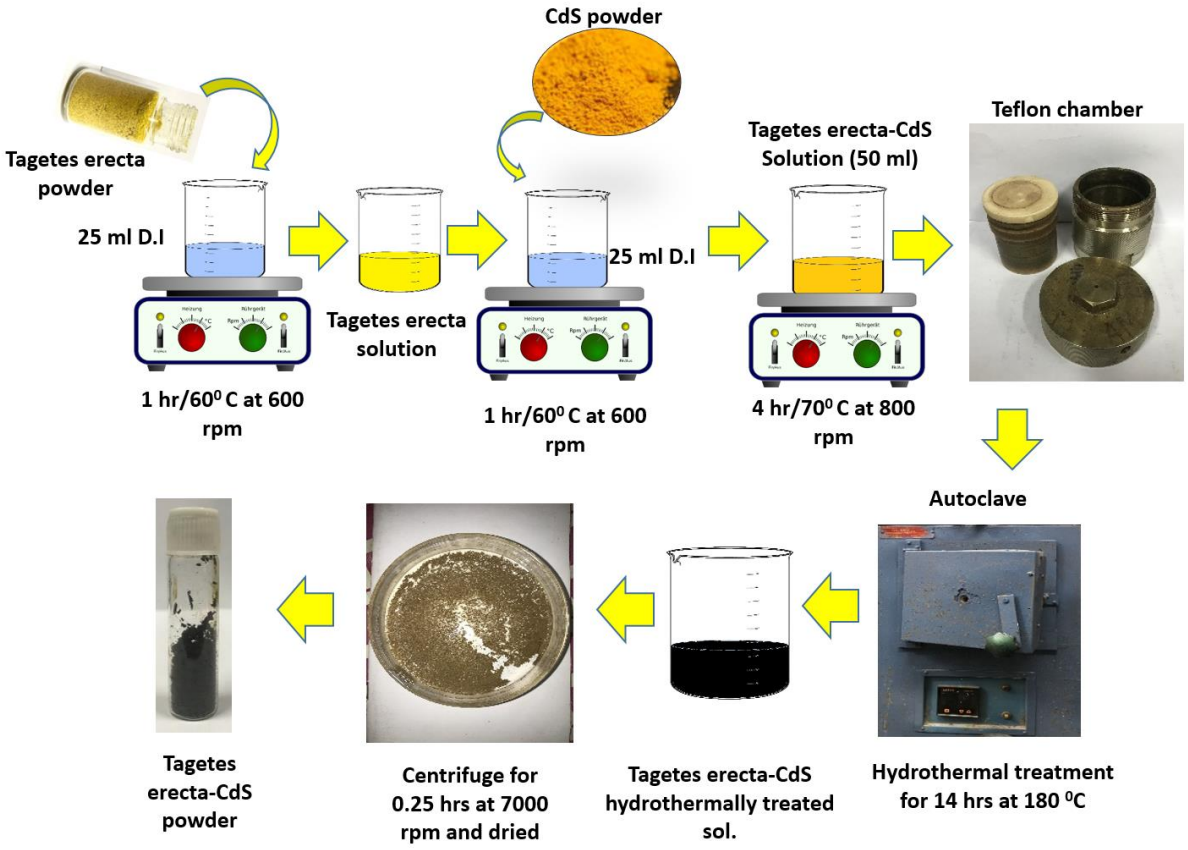


Fig 2.4: Schematics of Tagetes erecta-CdS powder synthesis.

115 gm of the synthesized Tagetes erecta powder is dissolved in 25 ml D.I. water and mixed with vigorous stirring and heating at 600 rpm at 60^0 C in a dark condition for 1 hour. Similarly, CdS 0.112 gm is dispersed homogeneously in 25 ml D.I. using magnetic stirring method for 1 hour at 600 rpm at 60^0 C. Finally, the CdS solution is added to the Tagetes erecta solution and continuously stirred for 4 hours/60^0 C at 800 rpm. The obtained mixture is continuously stirred at 800 rpm at 70^0 C with a rate of heating 2^0 C.min^{-1}. The final resulting solution obtained is treated hydrothermally in an autoclave for 14 hours at 180^0 C. Resulting Tagetes erecta-CdS solution has been washed multiple times, purified, dried, and stored in vacuum chamber.

2.6 Characterization of Samples

2.6.1 Structural Characterization:

2.6.1.1 X-ray Diffraction (XRD):

X-ray diffraction is a scientific technique which is used for material analysis. This technique is used to quantify and characterize the constituents of minerals, which provide the source information of raw material. XRD data is used to determine the manufacturing, alteration, and uses. The powder XRD method is done by using Bragg's law. X-rays produced from the cathode ray tube are focused monochromatically radiation towards the sample.

Bragg's law states that angle of incidence and angle of scattering of X-rays are equal when striking a crystal surface. Additionally, constructive interference happens when path difference is equal to wavelengths, where n = 0, 1, 2, 3, 4……., n[37].

Bragg's law mathematical equation:

$$n\lambda = 2d \sin \theta \qquad (2.1)$$

Where; d = Path difference, θ = Incident angle[38].

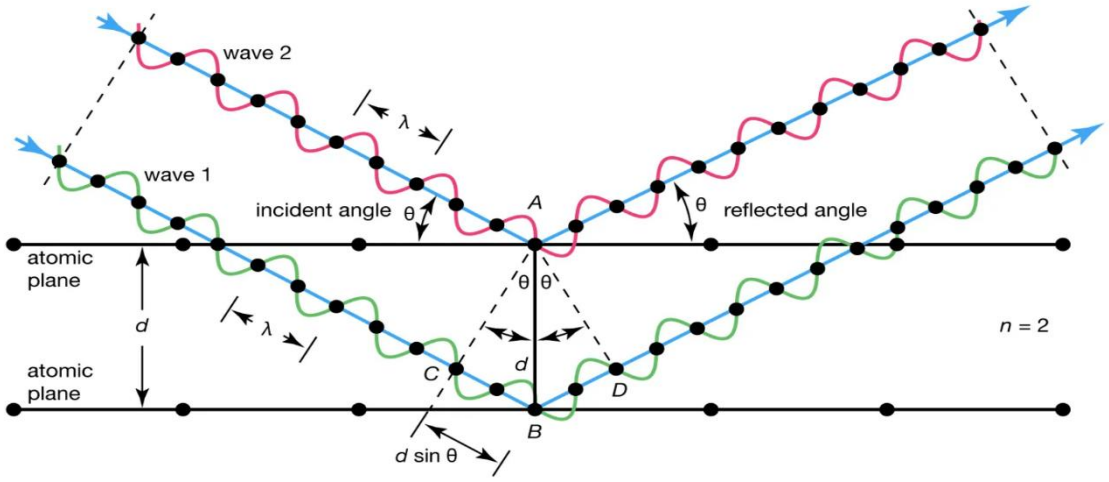


Fig 2.5: Bragg's diffraction.

Britannica, The Editors of Encyclopaedia. "Bragg law". Encyclopedia Britannica, 6 Feb. 2024, https://www.britannica.com/science/Bragg-law. Accessed 19 May 2024.

2.6.1.2 Fourier Transform Infrared (FTIR) Spectroscopy:

FTIR is a method that determines inorganic, organic, and polymer-based materials according to infrared light absorption characteristics. In comparison to traditional spectrometers, FTIR provides a faster-infrared spectrum. Fig 2.6 shows the major component of a basic Fourier transform infrared spectrometer. During analysis, an IR beam is emitted from the source, and then the beam goes to the interferometer where the encoding of IR spectral takes place. An interferogram has been generated due to the recombination of IR beams of different path lengths. The interference involved in the interferogram is destructive and constructive interference. Then the IR beam goes to the compartment of a sample where absorption of specific wavelength energy takes place. The interferogram has been generate according to the characteristics of the sample. The detectors finally measure all the frequency signals in the form of Energy vs. time. Using special software final data has been collected in the form of CSV format that helps to plot a graph of intensity vs. wavenumber[39].

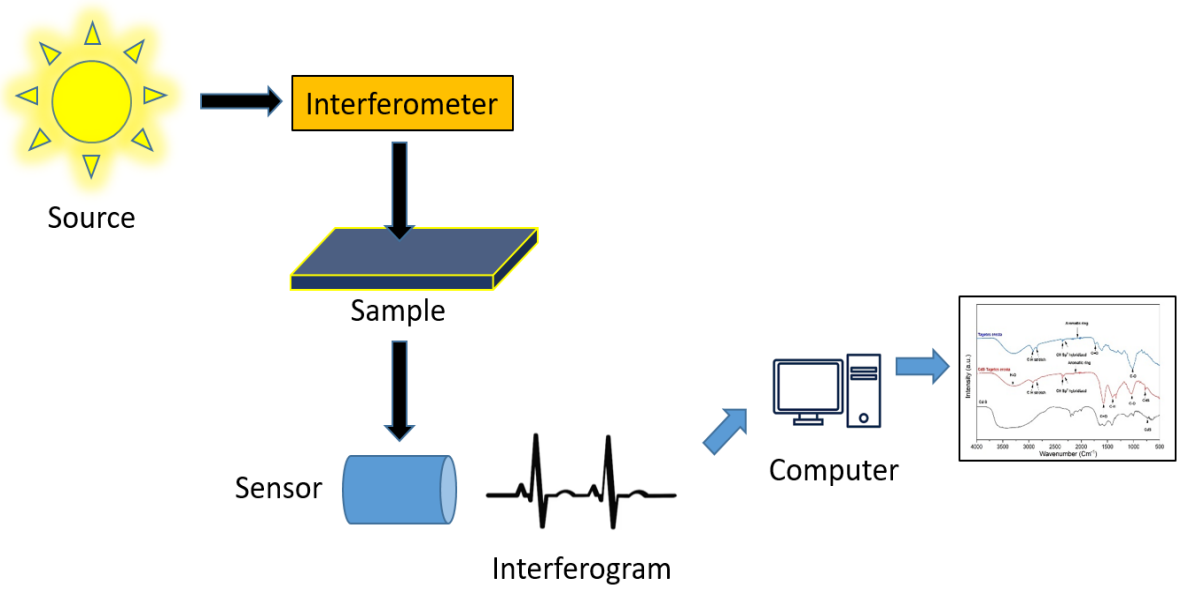


Fig 2.6: Schematic of 'Fourier Transform Infrared' analysis.

2.6.1.3 Thermogravimetric analysis-TGA:

It is a technique that involves quantitative analysis which monitors the sample mass from a range of 1 gm to several gm with furnace temperature up to 1600 ^{0}C. TGA measures sample temperature, mass, and time. The program made for temperature analysis includes cooling, heating, a combination of them, or isothermal holds. TGA contains a sample pan with a precise micro balance with a controller-thermo balance and temperature programmer.

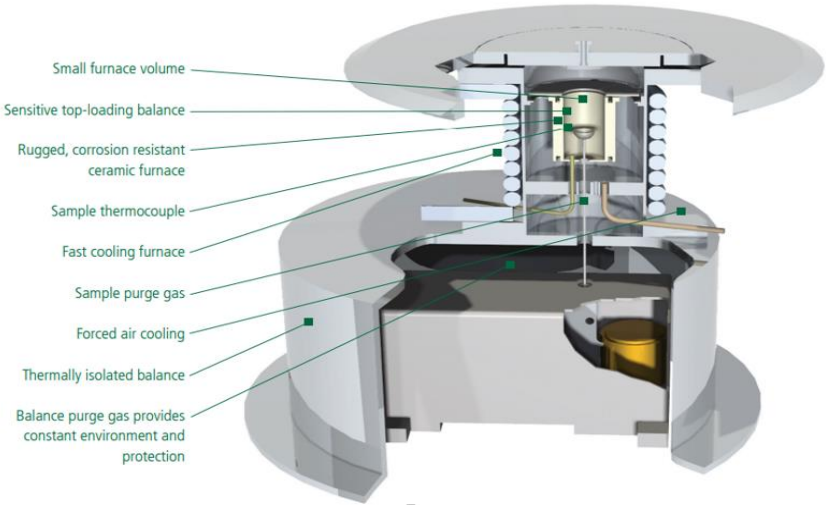


Fig 2.7: Thermogravimetric analysis[40].

2.6.2 Morphological Characterization:

2.6.2.1 Field Emission-Scanning Electron Microscope:

It is a kind of electron microscope that contribute ultra-high imaging resolution at low voltage and small distances. The system contains various types of sensors/detectors for the detection of various signals which covers various applications such as top surface imaging and analysis of elements of nanopowder. The images provide a resolution as low as 1.2-0.6 nm at a provided voltage of 1-15 KV.

- The detectors involved in FE-SEM are:

Detectors	**Work**
➢ Secondary electron (SE)	Topographic information

➢ Back-scattered electron (BSE)	Material composition contrast
➢ Energy dispersive X-ray spectroscopy (EDS)	Chemical composition (Energy resolution < 129 eV, detection limit 1000-3000 ppm)
➢ Wavelength dispersive X-ray spectroscopy (WDS)	Chemical composition (Energy resolution < 2-20 eV, detection limit 30-300 ppm)

Table 2.3: Field Emission-Scanning Electron Microscopy parts and their works.

2.6.2.2 Energy dispersive X-ray spectroscopy (EDS):

EDS is a method for examining the chemical composition of a specimen. When x-ray photons hit a detector, because of knocking out electrons, a very low amount of current gets produced from a semiconductor. The electrons emitted from the silicon electron shell absorb a specific energy of an element. The current generated from each X-ray photon and the original X-ray photons get compared and calculated using this method elements get identified[41].

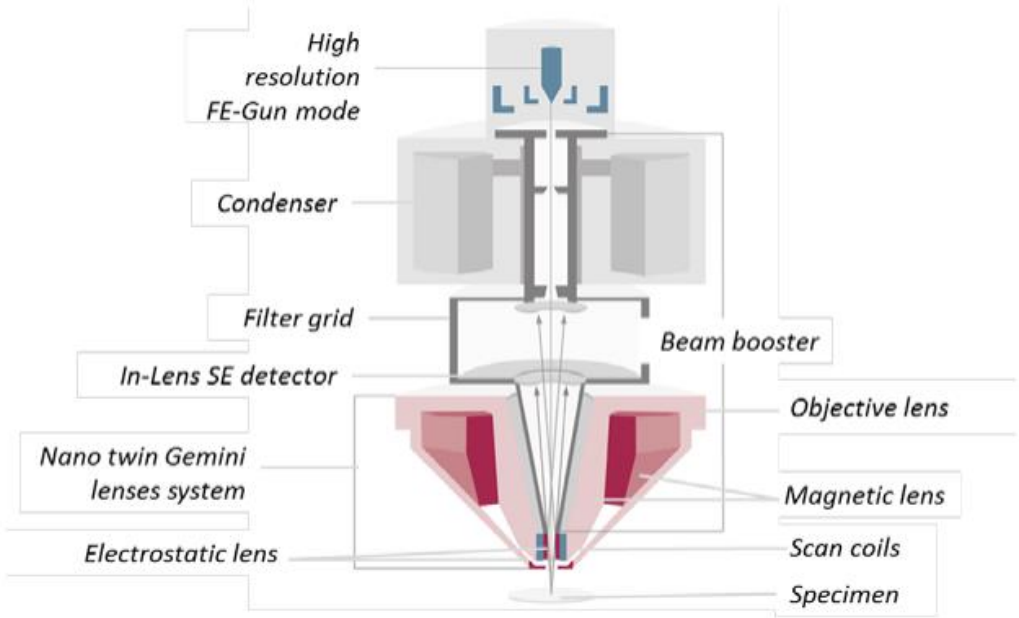


Fig 2.8: Schematic diagram of different parts of Field Emission-Scanning Electron Microscopy[40].

2.6.3 Electrochemical characterization:

2.6.3.1 Transient Photocurrent:

The transient photocurrent is used to study charge extraction generated by the photovoltaic effect as a function of time. A film of semiconductor coated on the glassy electrode. The film of a semiconductor gets excited when a pulse of light is provided on it. The generated photo charges get extracted on a glassy electrode, resulting in a current, and can be displayed by the source meter in the form of graph [42].

2.6.3.2 Linear sweep photo voltammetry (LSV):

This method is based on voltammetry where the current is calculated at the working electrode. In this method, a layer of semiconductor coating is done on the electrode (Working electrode). This method uses varying potential difference (swept stepwise in time) across the reference electrode and working electrode. The peak can be observed when species start to reduce or oxidize[43].

2.6.3.3 Cyclic voltammetry:

Cyclic Voltammetry is an electrochemical technique; it measures the current developed in an electrochemical cell under conditions where voltage is in excess of that predicted by the Nernst equation. CV is performed by cycling the potential across a working electrode and counter electrode with respect to the reference electrode, and measuring the resulting current.. It is used to determine oxidation and reduction of molecular species. CV can also be used to study the performance of electrodes and the characterization of the mobility of electrons[44].

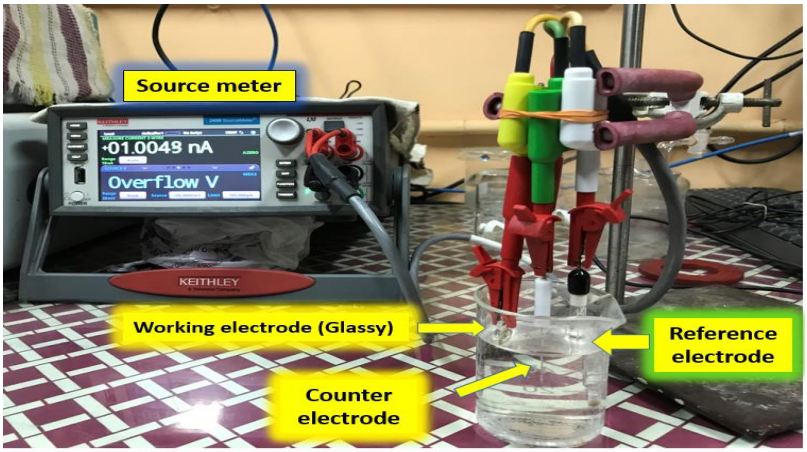


Fig 2.9: Setup of Transient photocurrent, Linear Sweep Voltammetry, and Cyclic Voltammetry.

2.6.4 Optical characterization:

2.6.4.1 Ultraviolet-visible Spectroscopy (UV-Vis):

UV-Vis spectrophotometry is used to study absorbance or transmittance of the sample. It measures the light absorbance within the range of ultraviolet and visible regions of electromagnetic spectrum. UV-visible spectrophotometer (Lambda 365) is a device used for UV-Vis spectrometry. This device can be used to study different types of samples such as gases, solids, and liquids by applying radioactive radiation within or near the range of visible (λ = 380-780 nm), and ultraviolet (λ = 170-380 nm) electromagnetic spectrum.

This method works on the principle of Bouguer-Lambert-Beer law.

$$\mathbf{Ln\ (I_o/I)_v = A_v = \varepsilon_v * C * d = ln\ (100/T(\%))_v} \qquad \mathbf{(2.2)}$$

Where;

$\mathbf{A_v = ln\ (I_o/I)_v}$ is the absorbance,

$\mathbf{T_v = (I/I_o)*100}$ in % is the transmittance,

$\boldsymbol{\varepsilon_v}$ = Molar decadic extinction coefficient/ absorptivity,

$\mathbf{I_o}$ = Monochromatic light intensity entering the sample,

C = Concentration of sample,

d = Path length in cm,

$\boldsymbol{\lambda}$ = Wavelength (nm)[45].

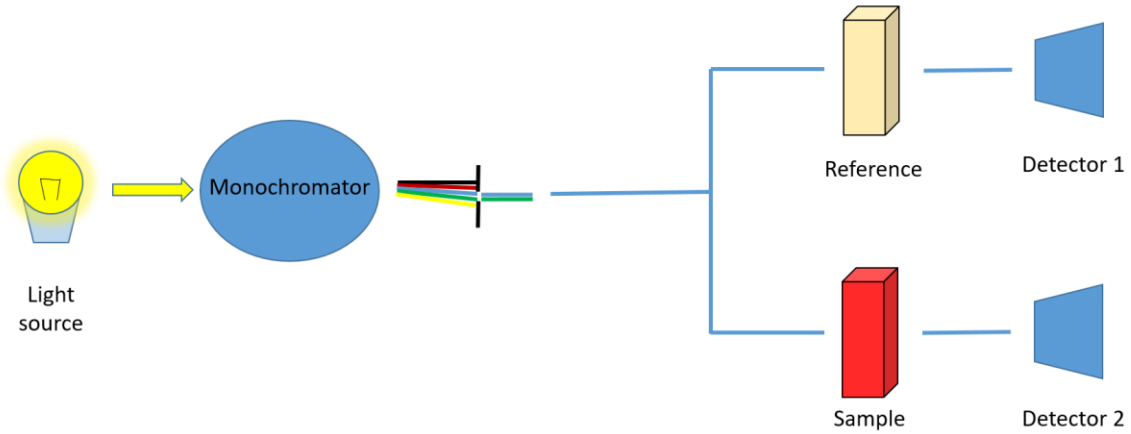


Fig 2.10: Schematic of 'Ultraviolet-visible Spectroscopy.

2.6.4.2 Tauc Plot:

Tauc plot is a graphical process for calculating optical band gap of insulator or semiconductor. The process involves analysing an absorption coefficient (α) of material in relation to photon energy (hv). This plot is named after Jan Tauc, who created this method

Mathematical expression;

$$(\alpha.h.\lambda)^2 = B(h.\lambda - Eg) \qquad (2.2)$$

Where,

α = Absorbance;

h = Planck constant;

λ = Photon's frequency;

B = Constant;

Eg = Bandgap energy[45].

2.6.4.3 Photoluminescence spectroscopy (PL):

PL is an optical characterization method in which a sample acts as a body that first absorbs photons and then radiates photons again. Quantum mechanics explains that the excited electron with higher energy is followed by a return to its initial state with lower energy and emits photons. Electrons only move to conduction band from valance band when sufficient amount of energy is supplied (Greater than bandgap energy) which is absorbed by the particle. Photoexcitation can make an electron have high energy then it loses its energy to come to rest in the conduction band. The process of emission and excitation of photons is known as photoluminescence.

PL emitted is directly proportional to the amount of relative recombination rates. If the sample is pure (contaminants free), then the recombination of conduction band electrons and valence band holes , and as a result small binding energy excitation has been observed between conduction and valence band. When the sample is contaminated or doped, recombination of electron-hole pair occurs via shallow level of donor-acceptor. PL helps to analyse the energy transfer, band gap, and impurity in the sample[46].

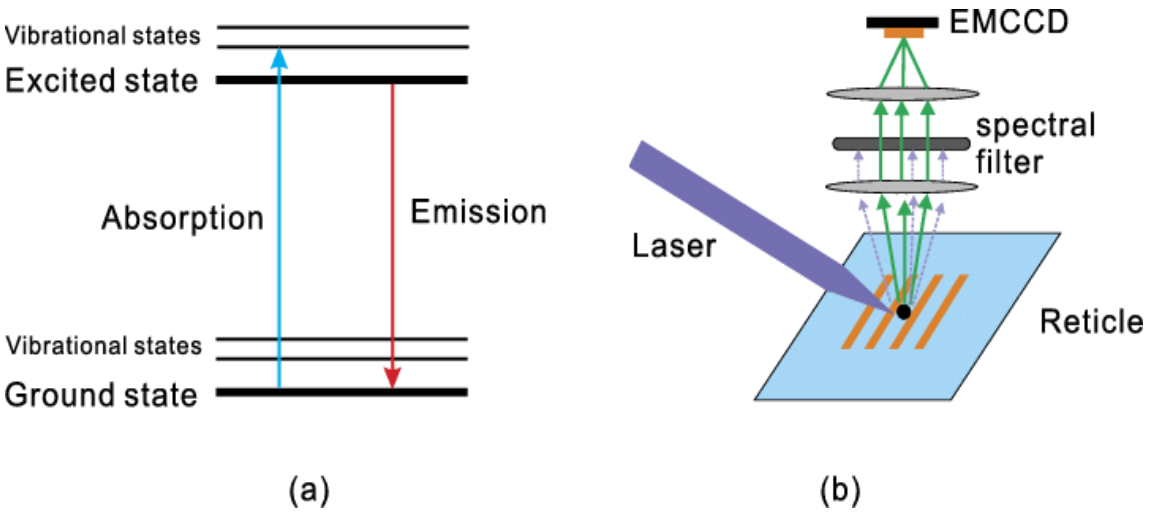


Fig 2.11: Principle of photoluminescence spectroscopy[47].

2.7 Solar simulator:

A Solar simulator can be defined as a device that can be used as an artificial sun as the source of light for laboratory-scale experimental purposes. It provides the same spectral composition and intensity as natural sunlight. A 100 W Solar simulator (94011A, Manual shutter, Newport Oriel LCS-100), equipped with an AM 1.5G air mass filter, was used. The AM 1.5G filter fitted into the LCS-100 solar simulator (Class ABB) can achieve class A spectral performance in accordance with the 1 sun irradiance output defined by IEC and ASTM standards. Experiments were performed using the full band spectrum of the solar simulator and bandpass filters at 420 nm.

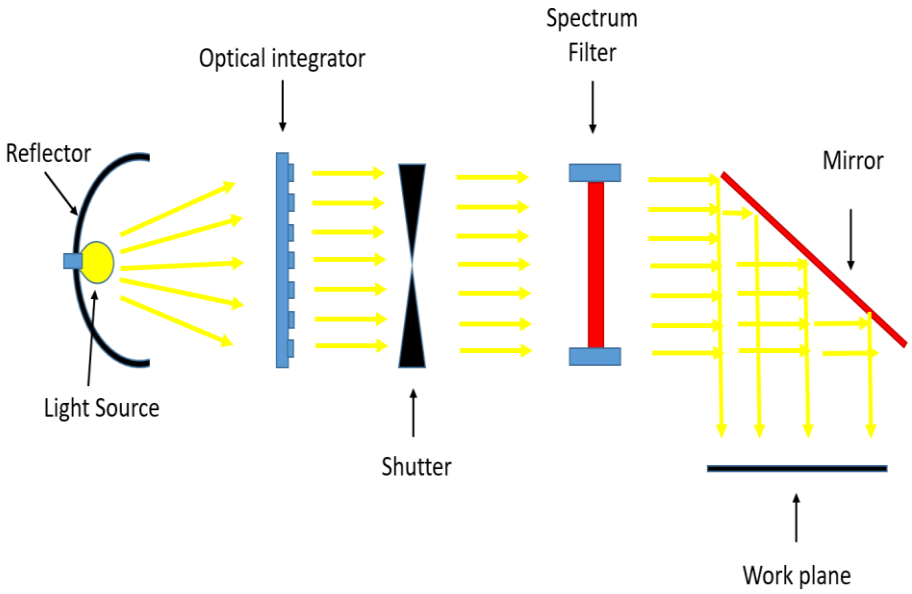


Fig 2.12: Working principle of the solar simulator.

2.7.1 **Bandpass filter:**

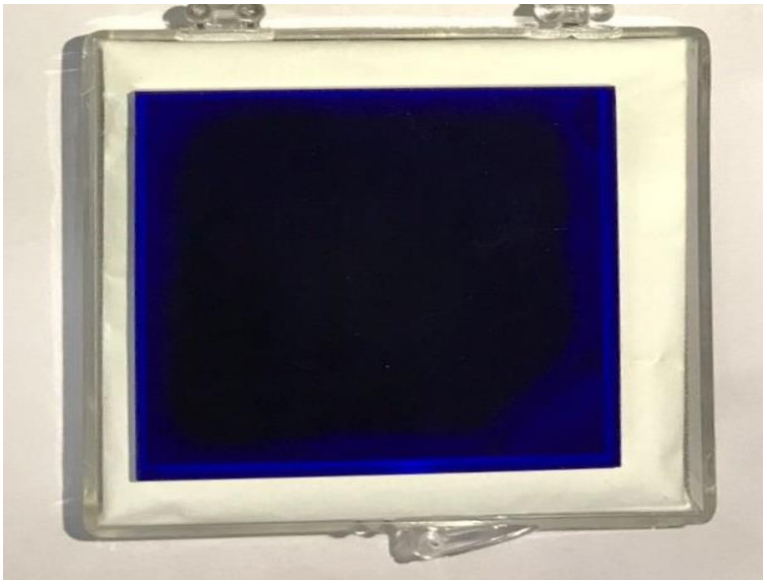


Fig 2.13: 420 nm Band Pass Filter.



Fig 2.14: Newport LCS-100 solar simulator[48].

2.8 Photocatalytic Hydrogen generation experimental set-up:

The Photocatalytic Hydrogen generation experimental setup consists of various parts such as:

1. Solar Simulator (Newport LCS-100 ABB class)
2. Glass based fabricated hydrogen generation reactor.
3. Control Valve for minimising gas leakage.
4. Hydrogen gas outlet.
5. Water Displacement Unit for Hydrogen volume measurement.
6. Power meter.

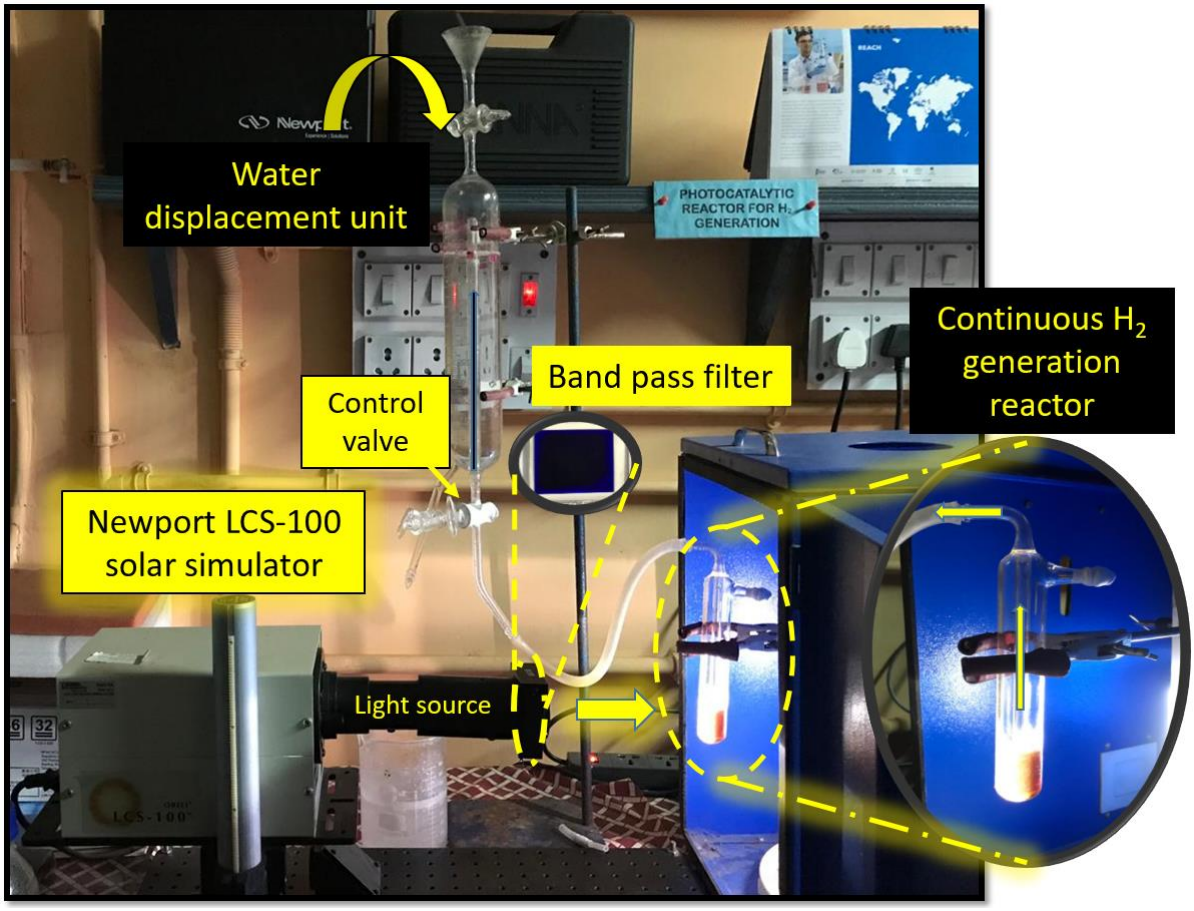


Fig 2.15: Setup of photocatalytic hydrogen generation.

2.9 Study of Hydrogen Generation:

2.9.1 Performance Study:

During the experiment 0.05 g Tagetes erecta-CdS and 0.01 g Sodium sulfide dispersed in 10 ml deionized water and stirred continuously for 1 hr. A solar simulator of Newport Oriel LCS-100 with air mass filter (AM 1.5 G) has been used to get one solar sun intensity (113 mw/cm^2), after stirring photocatalyst was put inside the reactor for photocatalytic reaction for up to 6 hrs. For initializing the process**,** photocatalytic reactor and water displacement unit are kept under vacuum using a vacuum pump. Light comes from the solar simulator when irradiates on the surface of the reactor, the catalyst loaded in it starts the photocatalytic reaction, and the hydrogen generated during this reaction gets collected in the water displacement unit. The cumulative hydrogen generated versus time is obtained and from the slope of the curve the rate of hydrogen generation is evaluated. Experiments are performed using full band spectrum of solar irradiation and using 420 nm band pass filter.

2.9.2 Performance Analysis:

Below performance analysis has been done during this experiment to measure the photocatalytic function.

1. **Activity of photocatalyst**

   Water displaced during this experiment is used to calculate the amount of hydrogen generated in moles. The displaced volume in ml. gets converted into millimole. The moles of hydrogen generated per unit time per unit gm. of catalyst is called photocatalytic activity. Photocatalytic activity of a catalyst can be determined the productivity quality of the catalyst.

$$\textbf{Activity} = \frac{\boldsymbol{Moles\ of\ generated\ hydrogen(mmol)}}{\boldsymbol{photocatalyst\ (gm.) * irridiation\ time\ (hr)}}$$

2. Apparent Quantum Yield (AQY)

The ratio of emitted photons number to the absorbed photons number is known as apparent quantum yield. The energy of photons can be calculated as the photon of a specific energy absorbed to initiate the water-splitting photocatalytic reaction. The equation used to calculate the energy of photons is given below [44]:

$$E_{Photons} = \frac{hc}{\lambda}$$

Were,

$E_{Photons}$ = Photons energy in joules (J);

h = $6.6260715 \times 10^{-34}$ J.s (Planck's constant);

c = 3×10^{8} m/s (Speed of light);

λ = Wavelength of photons in meters (m).

The monochromatic light total energy has been calculated using following equation:

$$E_{Total} = P.s.t$$

Were,

P = Power density of monochromatic incident light (W/m^2),

s = Exposed area to irradiation (m^2),

t = Exposer time to incident light (s).

So, Incident photons can be described as the ratio of E_{Total} to $E_{Photons}$. The mathematical equation is given below:

Number of the incident photons = $E_{Total} / E_{Photons}$

$$= \frac{P.s.\lambda.t}{h.c}$$

$$\mathbf{AQE}(\%) = \frac{\mathbf{2 \times The\ number\ of\ evolved\ Hydrogen\ molecules}}{\mathbf{The\ number\ of\ incident\ photons}} \times \mathbf{100}$$

$$= (2.\ n(H_2).N_A.h.c)/P.s.\lambda.t)\ X\ 100\ \%$$

Where;

$n(H_2)$ = Molecules of hydrogen evolved concern with time of incident light (mol).

N_A = 6.022 X 10^{23} mol^{-1} (Avogadro's constant).

3. Solar to Hydrogen Conversion Efficiency Calculation:

STH calculation is used to measure efficiency of photocatalytic splitting of water reaction of Solar to H_2 conversion efficiency. The mathematical expression used to calculate STH has been given below:

$$\frac{r_{H_2} \times \Delta G_{H_2O} \times 100}{I \times S}$$

r_{H_2} = Hydrogen evolution rate,

$\Delta G_{H_2O,}$ = Gibb's free energy,

I = Light energy flux,

S = Irradiation area[49]

Chapter-III

Result

&

Discussion

3.1 Structural characterization:

3.1.1 X-ray diffraction Analysis:

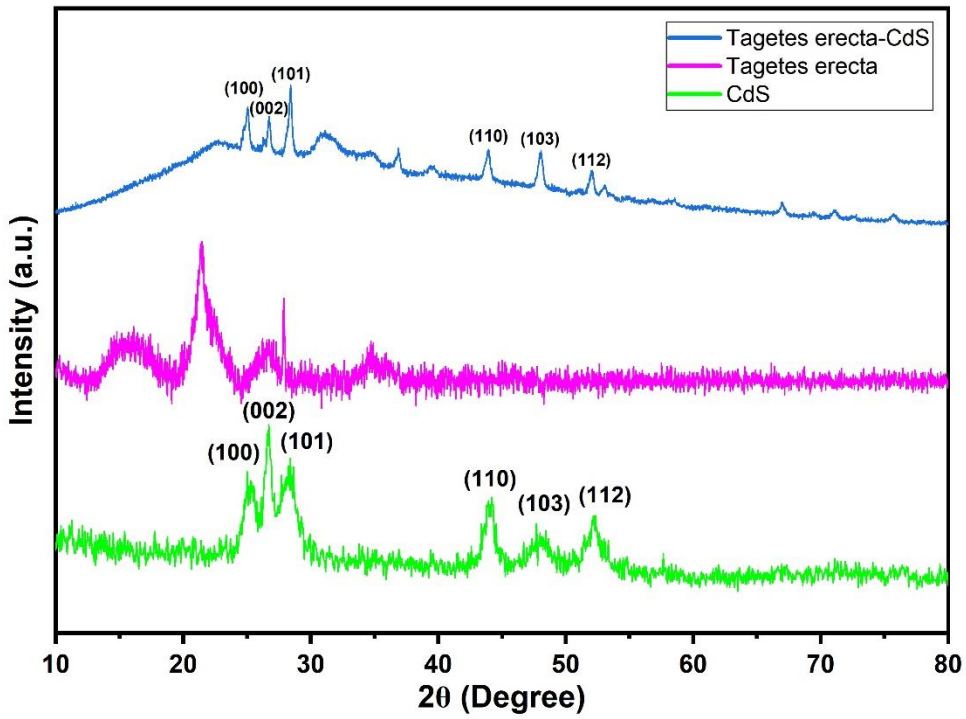


Fig 3.1: X-ray diffraction spectra of Tagetes erecta-CdS, Tagetes erecta, and Cadmium sulfide.

- Cadmium Sulfide nanoparticles display peaks at angles of 2θ: 25.06, 26.61, 28.32, 43.98, 48.06 and 52.16 attributing to (100), (002), (101), (110), (103) and (112) hexagonal wurtzite structure of the Cadmium sulfide crystalline planes of the Bragg's band angle at 2θ scale.
- XRD spectra of the hydrothermally treated Tagetes erecta-CdS photocatalyst displays the peaks at 2θ values 25.06^0, 26.61^0, 28.32^0, 43.98, 48.06^0, and 52.16^0 closely matching with (100), (002), (101), (110), (103) and (112) of hexagonal wurtzite structure of crystalline planes of Cadmium sulfide (JCPDS card No. 75-1545)[50] and the other peaks corresponding to the Tagetes erecta synthesized biomass.
- Addition of biomass to CdS causes the increase in the peak intensity of (100), (101), and (103); it signifies the enhancement of specific facets of CdS crystal.

3.1.2 Fourier-transform infrared spectroscopy Analysis:

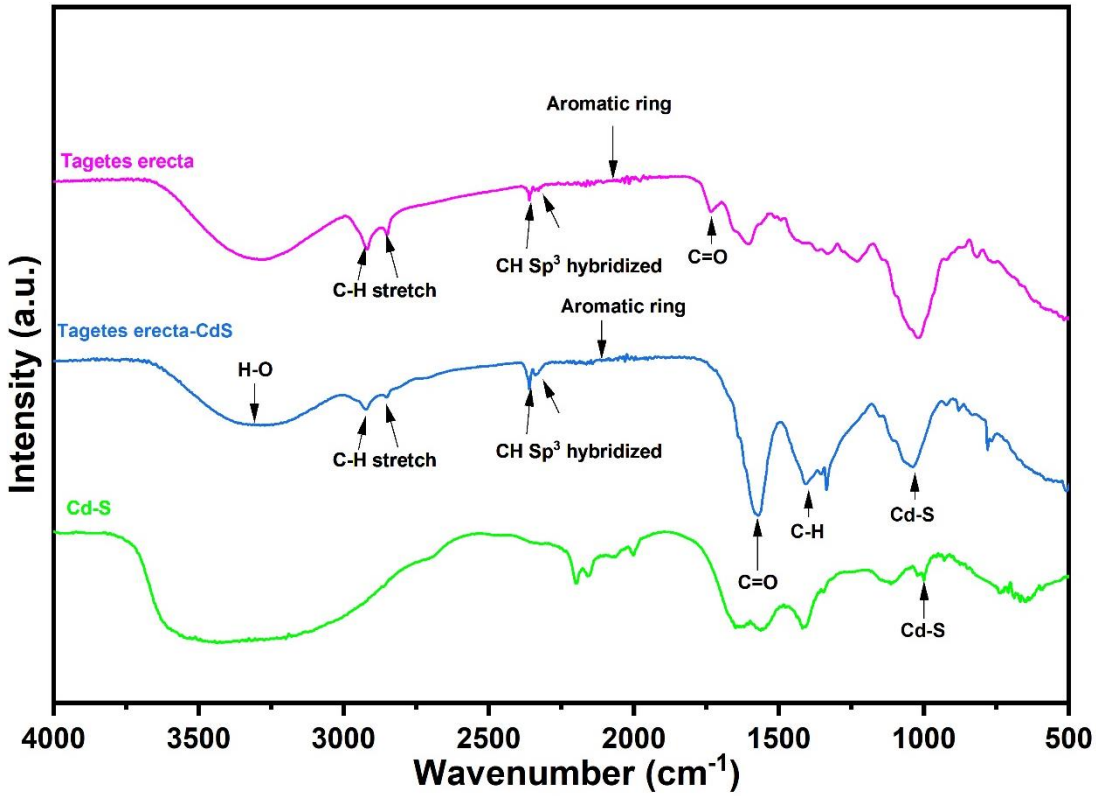


Fig 3.2: Fourier-transform infrared analysis of Cadmium sulfide, Tagetes erecta-CdS, and Tagetes erecta.

- In this Fourier-transform infrared spectroscopy graph different functional groups are associated with different peaks in a given infrared spectrum.
  a) Peak at 1000 cm^{-1} represent the stretching bond of Cd-S.
  b) 1403 cm^{-1} peak represent C-H bending vibrations in alkanes.
  c) Peaks around 1577 cm^{-1} and 1735 cm^{-1} represent C=O stretching vibrations in carbonyl groups.
  d) Stretching vibrations of C-H bonds in alkanes and aromatic compounds is denoted by peak at 2900 cm^{-1}.
  e) The peak at 2850 cm^{-1} of methyl group and methylene.
  f) 3306 cm^{-1}: The broad peak of this region represents the bending vibrations of the Water.

3.1.3 Thermogravimetric Analysis:

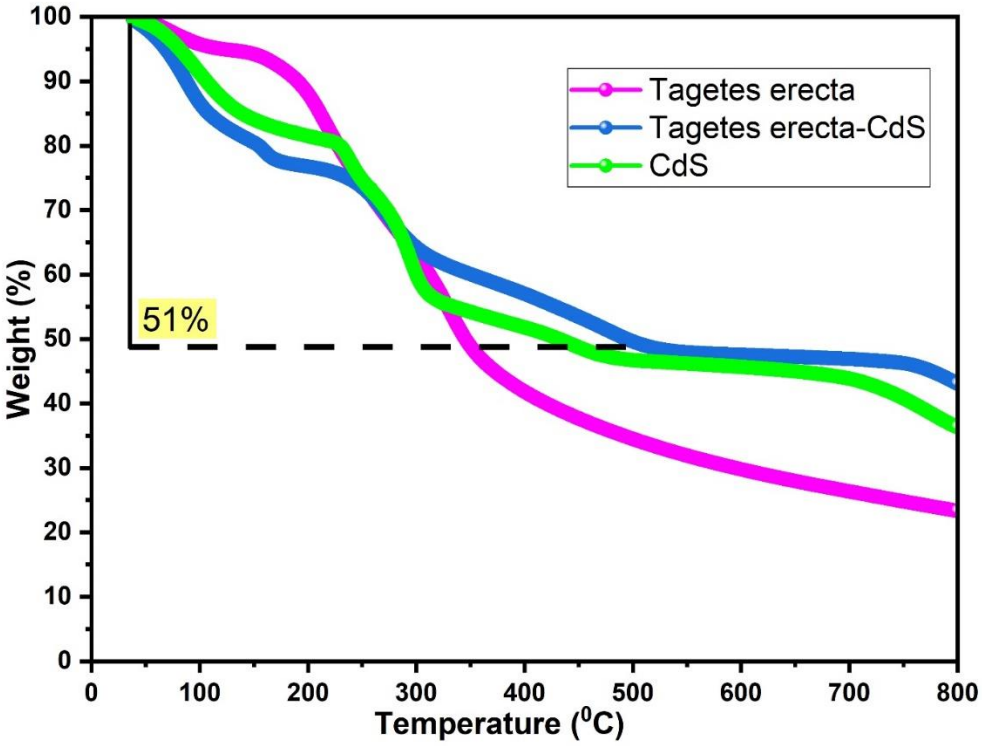


Fig 3.3: Thermogravimetric analysis of Cadmium sulfide, Tagetes erecta-CdS, Tagetes erecta.

Thermogravimetric analysis of Cadmium sulfide, Tagetes erecta-CdS and Tagetes erecta has been performed to determine the influence of thermal degradation on synthesized powder material. Thermal degradation and weight loss of synthesized powder have been occurred at three points in the range of 34 °C to 800 °C.

- The initial weight loss occurs in range of 34 °C to 162 °C as O-H functional groups begin to dissociate.
- A sudden slope decline is observed between 240 °C to 300 °C due to dissociation of bond between CdS and biomass.
- The third decay is observed between 300 °C to 595 °C due to thermal degradation of bond between Cd-S.

3.2 Morphological Characterization:

3.2.1 Field emission scanning electron microscopy Analysis:

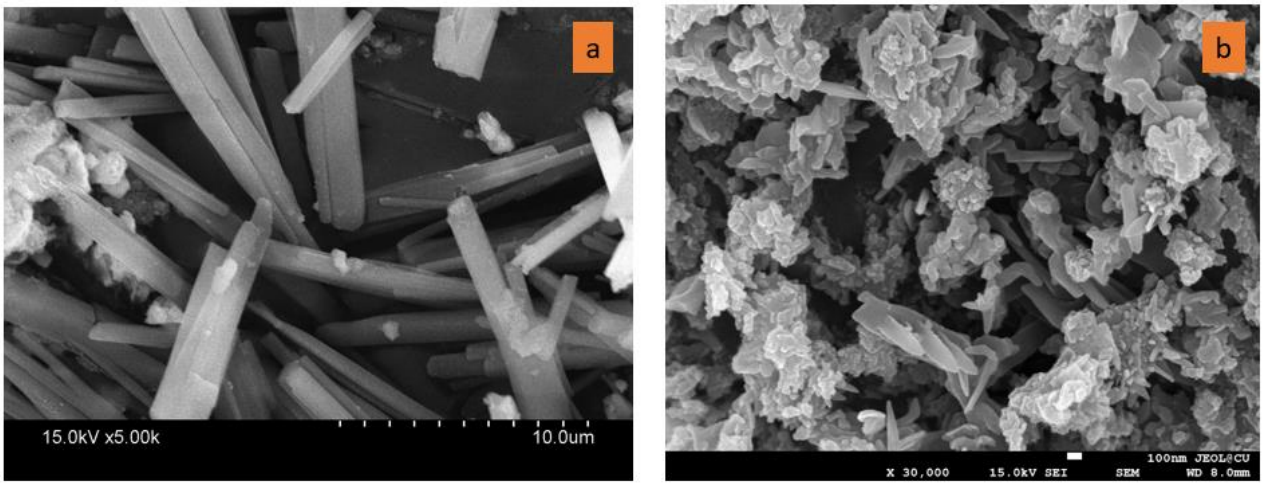


Fig 3.4: Field emission scanning electron microscopy analysis of Cadmium sulfide (a), and Tagetes erecta-CdS (b).

FE-SEM image Fig 3.4 (a) shows nano-rods with smooth surface area. Fig 3.4 (b) confirms the integration of CdS and Tagetes erecta, displaying formation of a layer of Tagetes erecta uniformly on the surface of CdS nanorod.

3.2.2 Energy-Dispersive x-ray spectroscopy analysis:

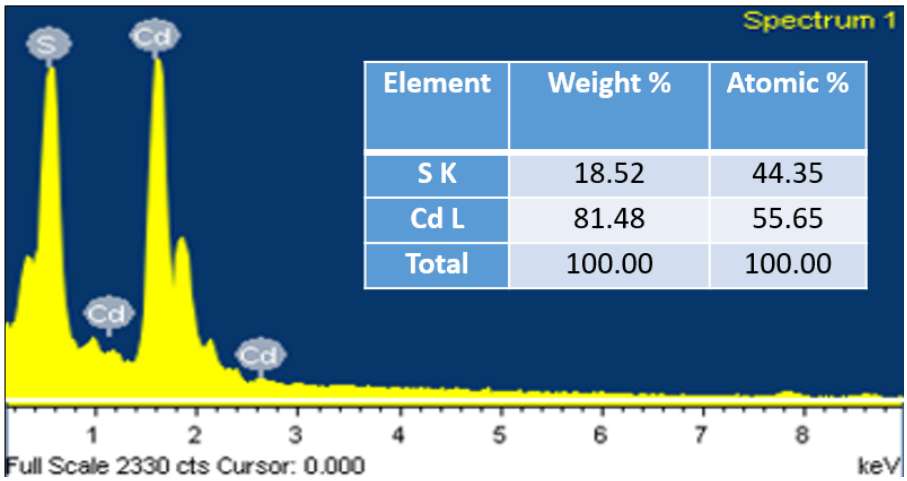


Fig 3.5 (a): Cadmium sulfide Energy-dispersive x-ray spectroscopy.

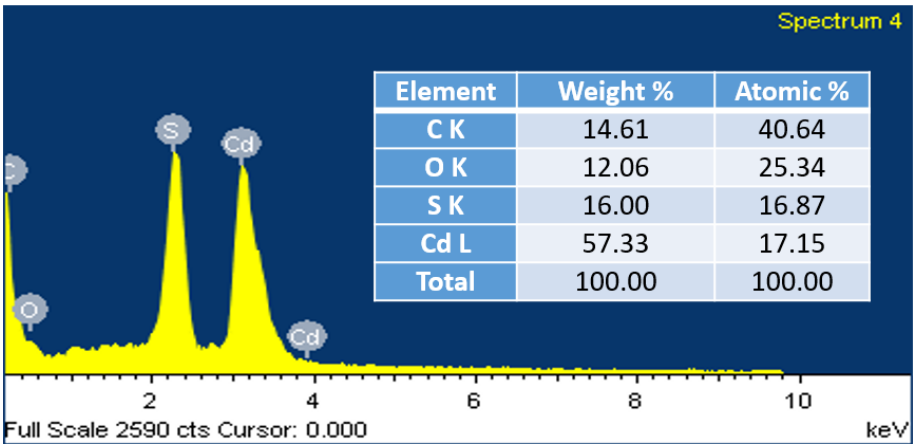


Fig 3.5 (b): Tagetes erecta-CdS Energy-dispersive x-ray spectroscopy.

EDS shown in Fig 3.5 (a) and (b) confirms the presence of elements namely Cadmium, Sulphur for pristine CdS and Carbon, Sulphur, Carbon and Oxygen in CdS-Tagetes erecta, respectively. There's a spike of Carbon (C) and oxygen (O) visible in the Fig.3.5 (b) which represent the biomass part of the synthesized material.

3.3 Optical Characterization:

3.3.1 UV-VIS Study:

Ultraviolet-visible spectroscopy is used to study optical absorption, here the optical absorbance of CdS, Tagetes erecta, and Tagetes erecta-CdS has been examined thoroughly. This UV-Vis study range of 170 nm – 780 nm of CdS-Tagetes erecta shows absorbance at 400.86 nm which corresponds to band gap of 2.24 eV. For CdS and Carotenoid, the peak has been observed at 524 nm and 416 nm, respectively.

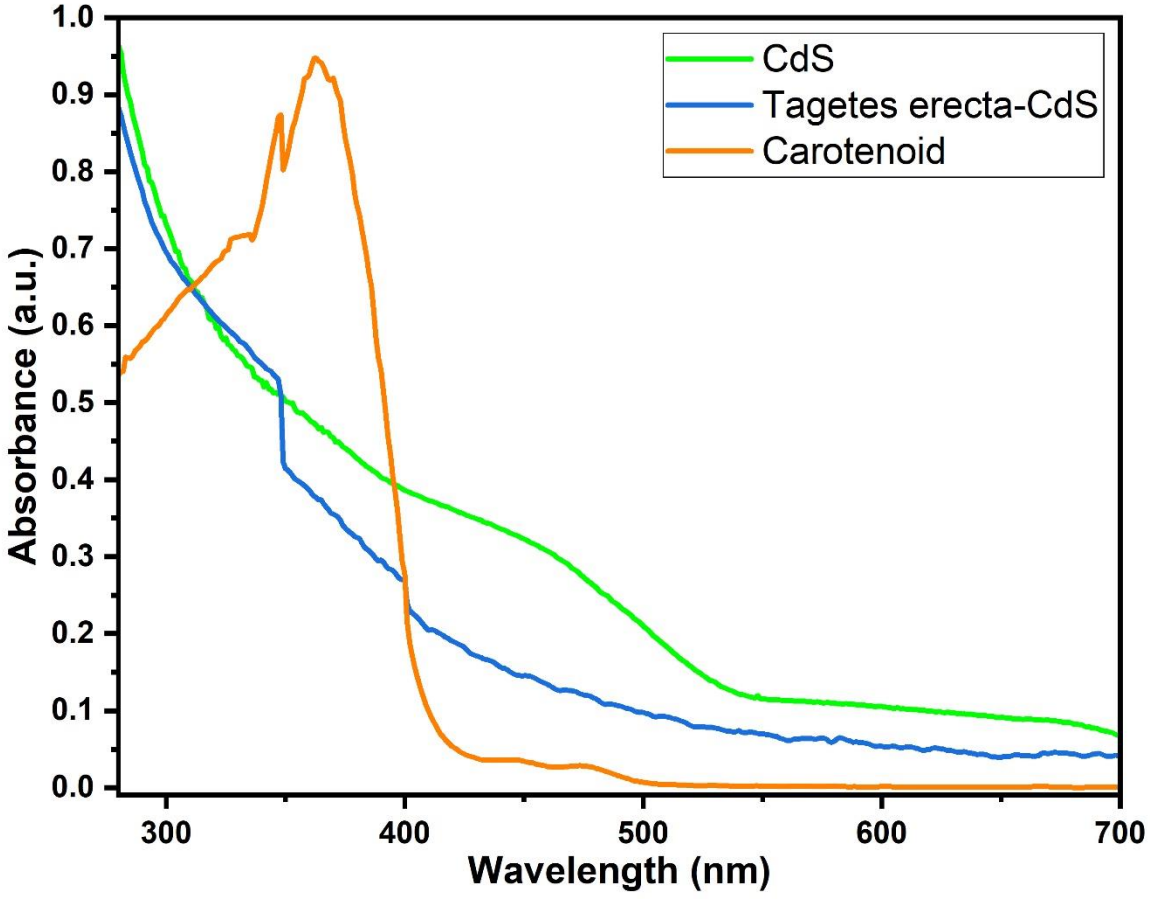


Fig 3.6: Ultraviolet-visible spectroscopy of Cadmium sulfide, Carotenoid, Tagetes erecta-CdS.

3.3.2 Tauc Plot:

The band gaps of the photocatalysts are measured using the tauc plot method. Pristine CdS, Carotenoid and Tagetes erecta-CdS exhibit bandgap of 2.48 eV, 2.60 eV, and 2.24 eV, respectively. The slope of $(\alpha h\nu^2)$ vs $h\nu$ gives the optical bandgap.

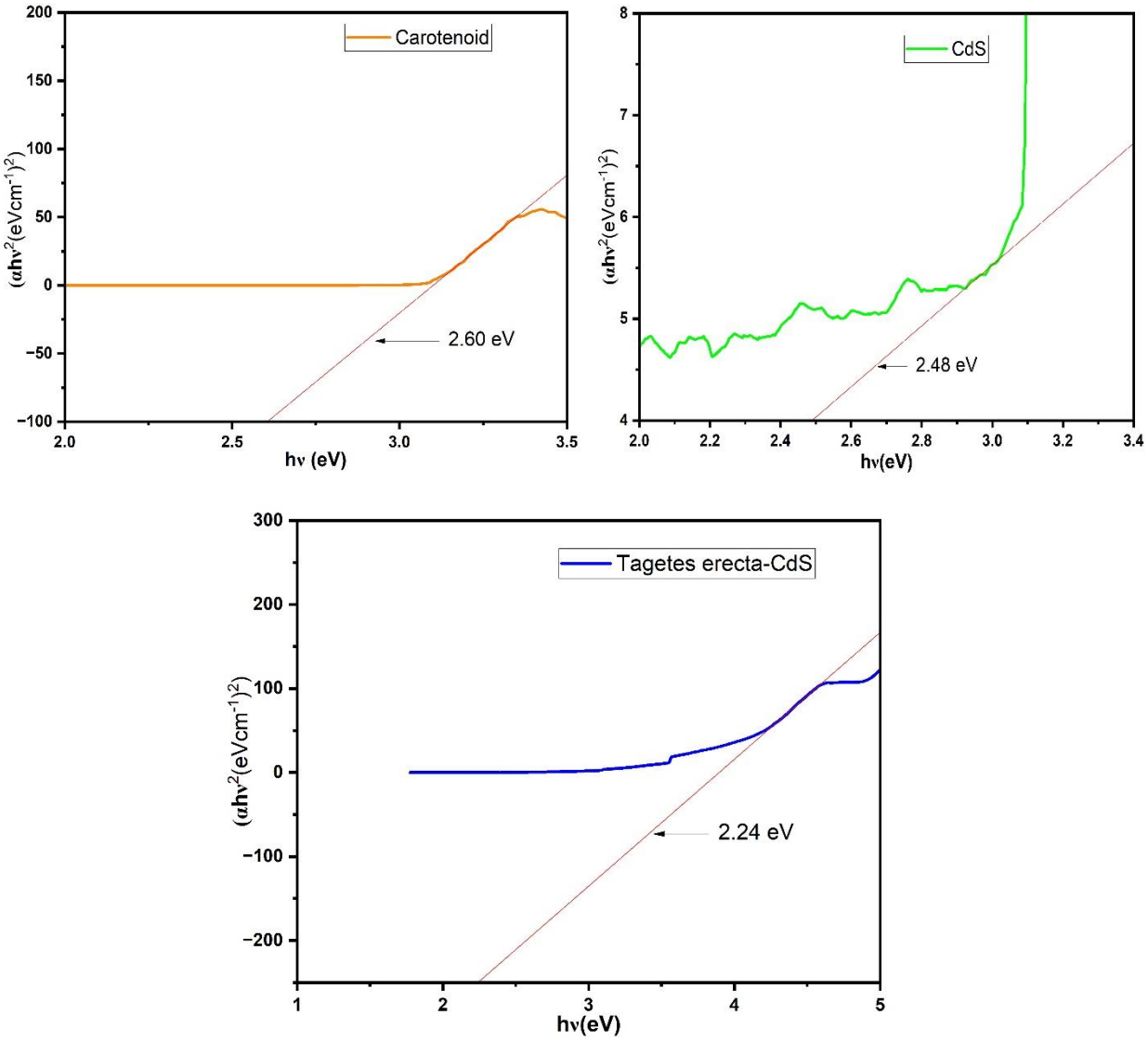


Fig 3.7: Tauc Plot for Band gap calculation of Cadmium sulfide, Carotenoid, and Tagetes erecta-CdS.

3.3.3 Photoluminescence (PL) Study:

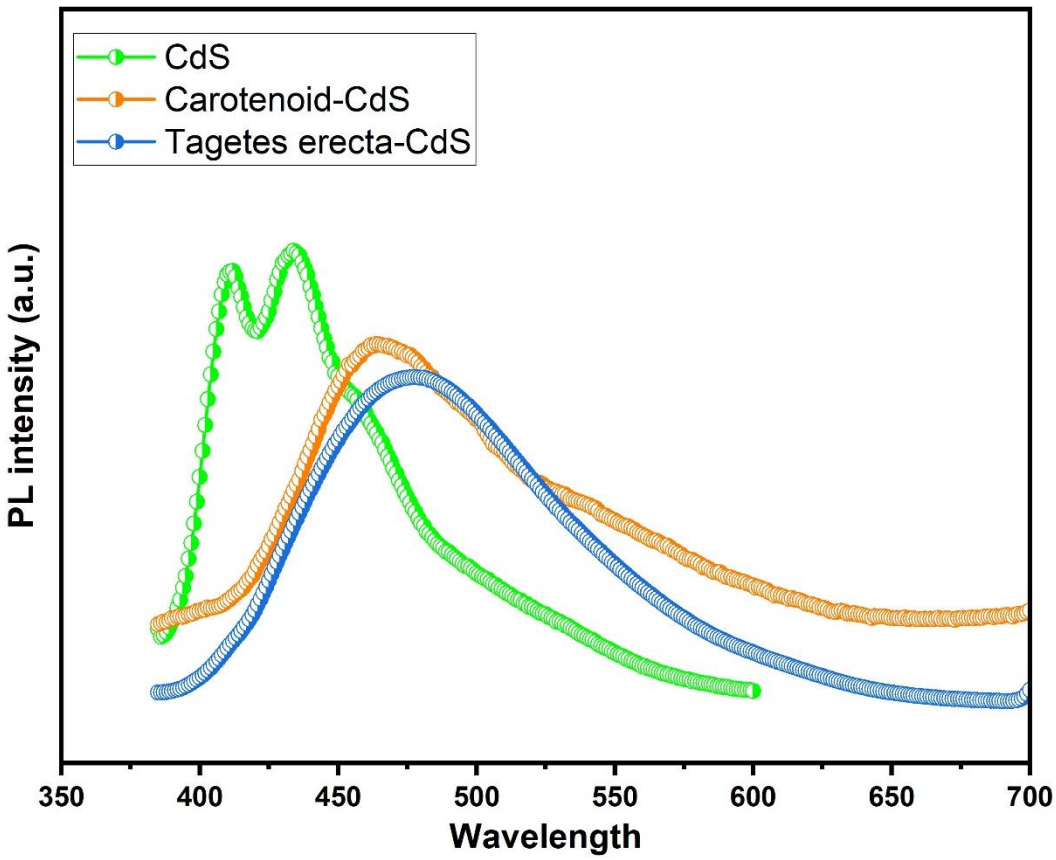


Fig 3.8: Photoluminescence analysis of CdS, Carotenoid-CdS, and Tagetes erecta-CdS.

Photoluminescence spectra of pristine CdS, Carotenoid-CdS and Tagetes erecta-CdS are shown in Fig 3.8. Tagetes erecta-CdS nanohybrid exhibits the lowest intensity among all three spectra, indicating the lowest recombination rate of photogenerated electron and hole pair.

3.4 Photo Electrochemical Study:

The photoelectrocatalytic properties were measured of prepared samples via Cyclic Voltammetry, Linear Sweep Voltammetry, and Photo Electric Current. All samples exhibit similar electro-oxidation characteristics.

3.4.1 Methodology of Glassy electrode coating:

A solution of isopropyl alcohol, deionized water, and Nafion in a ratio of **'200:50:50'** (µl) is made using the ultrasonication method, 5 mg of photocatalyst dispersed in the solution for 1 hour. The glassy electrode is then coated using the drop-casting procedure. A ½ M solution of Sodium sulfide anhydrous solvent is used as a medium for experiment and a 1 M solution of Potassium chloride is used for the reference electrode.

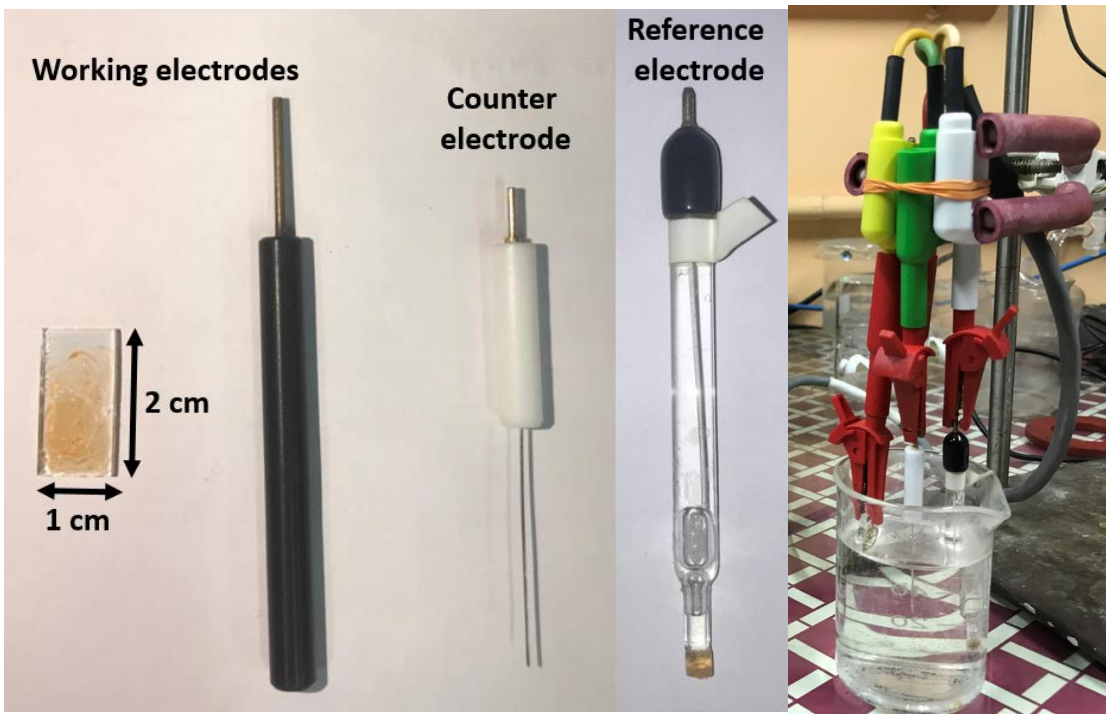


Fig 3.9: Setup of electrodes used for photocurrent, Cyclic and Linear sweep voltammetry analysis.

The working electrode is a glassy electrode and it is used for dropcasting. After dropcasting working electrode, counter electrode and reference electrode are placed in a homogenous mixture of 1/2 M sodium sulfide anhydrous. Photoelectrochemical reaction takes place between the working and counter electrodes.

3.4.2 Cyclic Voltammetry:

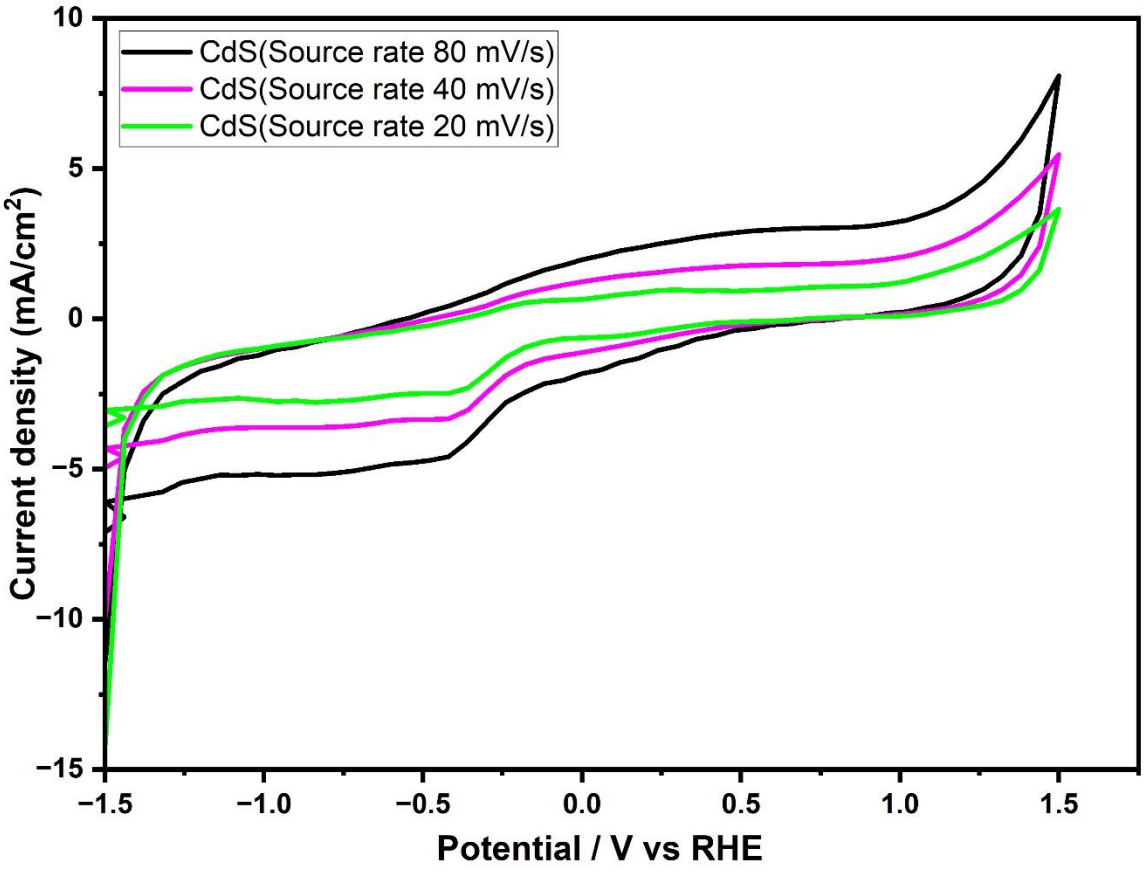


Fig 3.10: Cyclic voltammetry of Cadmium Sulfide with different Source rates.

Source rate	**Onset**		**Offset**	
(mV/s)	V	mA/cm^2	V	mA/cm^2
20	-1.398	-2.939	1.5	3.581
40	-1.445	-4.207	1.5	5.459
80	-1.449	-5.978	1.5	8.073

Table 3.1: Onset and offset values of Cadmium Sulfide with different source rates.

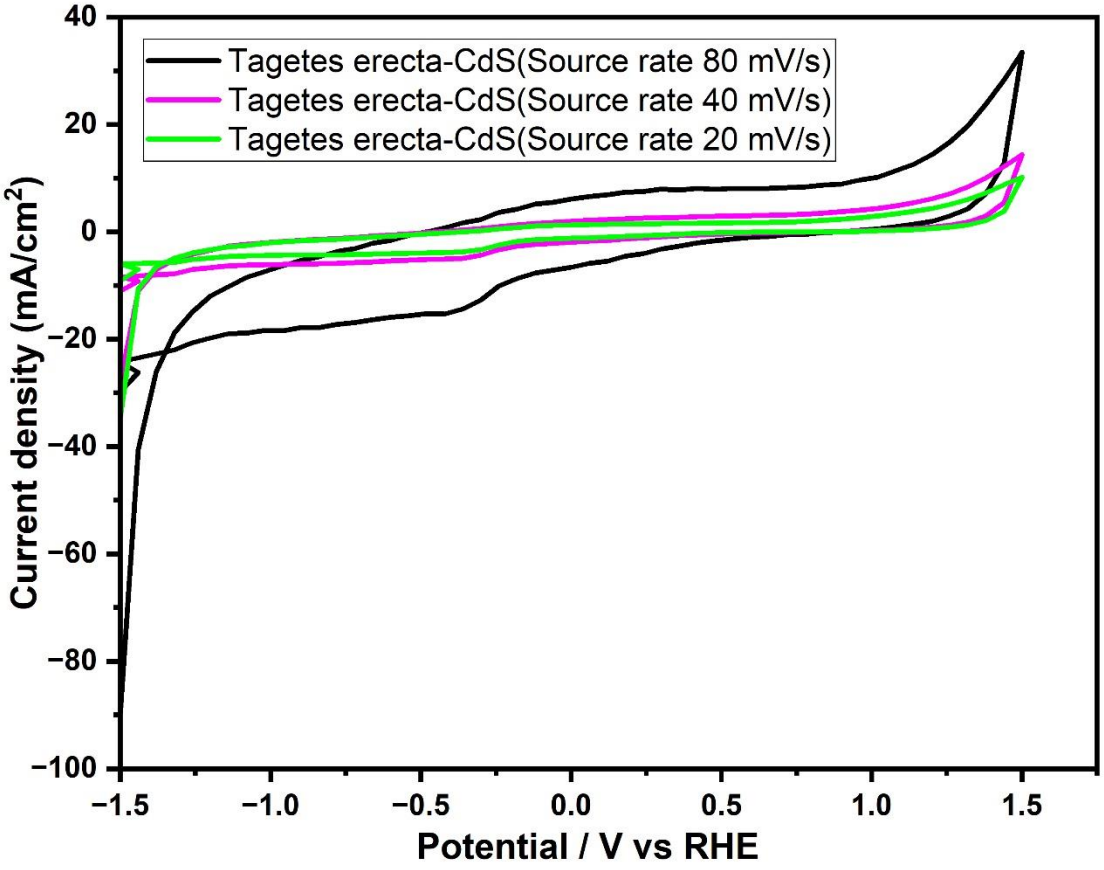


Fig 3.11: Cyclic voltammetry of Tagetes erecta-CdS with different Source rates.

Source rate	**Onset**		**Offset**	
(mV/s)	V	mA/cm^2	V	mA/cm^2
20	-1.356	-5.278	1.5	10.45
40	-1.389	-7.844	1.5	14.51
80	-1.35	-22.349	1.5	33.74

Table 3.2**:** Onset and offset values of Tagetes erecta-CdS with different source rates.

Cyclic voltammetry of CdS and Tagetes erecta-CdS is performed using source rates varying from 20 to 80 mV/s. Increasing the source rate from 20 to 80 mV/s leads to faster potential sweeps, affecting the electrochemical reaction kinetics. The peak shifting explains the changes in the redox processes happening on the electrode surface. Increasing the source rate increases the electron transfer kinetics at the surface of an electrode. The onset and offset potential and current density of CdS and Tagetes erecta-CdS for different source rates are given in the table 3.1 and 3.2.

3.4.3 Linear Sweep Voltammetry:

This Linear Sweep Voltammetry (LSV) plot shows the relationship between photocurrent density with respect to the applied potential of CdS and of Tagetes erecta-CdS:

1) Photocurrent response:
   a) The photocurrent density is very low at starting for both the samples.
   b) At the turn on potential, the photocurrent density starts to increase with respect to potential, which denotes the onset of photoelectrochemical activity.
   c) At a certain point potential photocurrent density reaches the maximum limit, indicating the occurrence of an optimal condition of photoelectrochemical processes.
   d) After attaining the maxima, it stabilizes at more positive values of potential.

   Turn on potential of CdS and Tagetes erecta-CdS observed as V_{oc} = -1.465 V, and V_{oc} = -1.367 V respectively. A sharp transition and increase in photocurrent densities are observed due to hydrogen evolution. Tagetes erecta-CdS from cathode to anode current in the comparison with another electrode. It may be informed that from LSV curve of Tagetes erecta-CdS shows better charge collection[51].

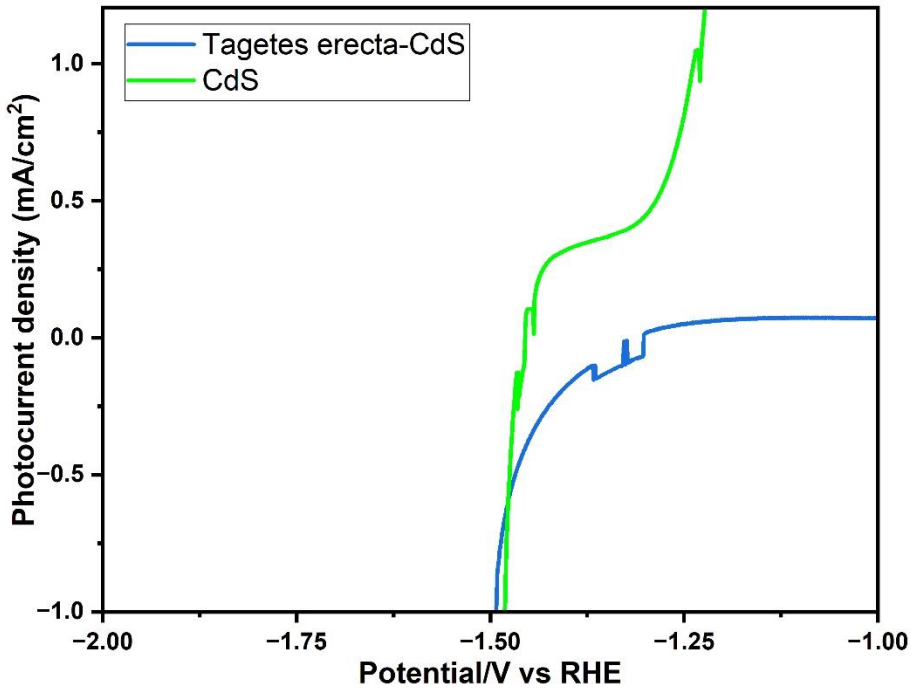


Fig 3.12: Linear sweep voltammetry of Cadmium sulfide, and Tagetes erecta-CdS.

3.4.4 Photo Current:

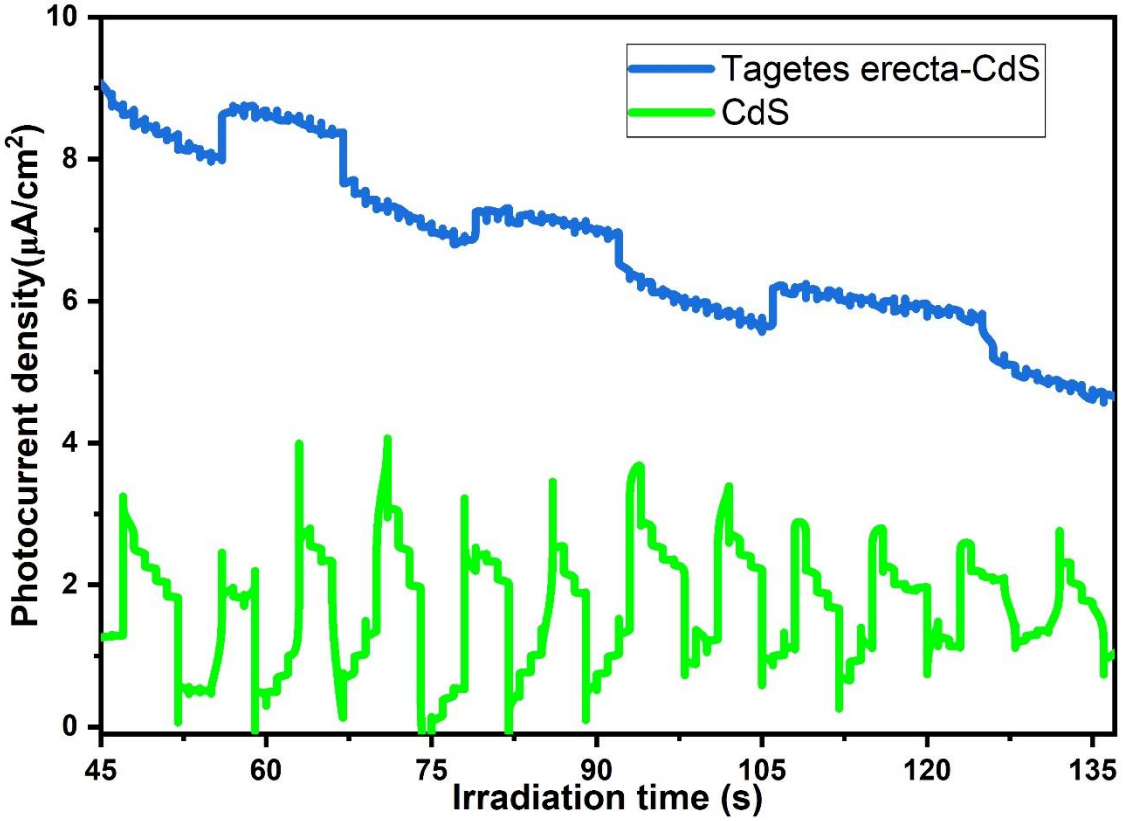


Fig 3.13: Photocurrent comparison of Cadmium sulfide and Tagetes erecta-CdS.

Fig 3.13 depicts the photocurrent density as a function of irradiation time. The higher value of photocurrent density exhibited by Tagetes erecta-CdS implies higher absorption rate of photons, enhancement in mobility and better charge transport.

3.5 Photocatalytic Hydrogen generation: Performance analysis:

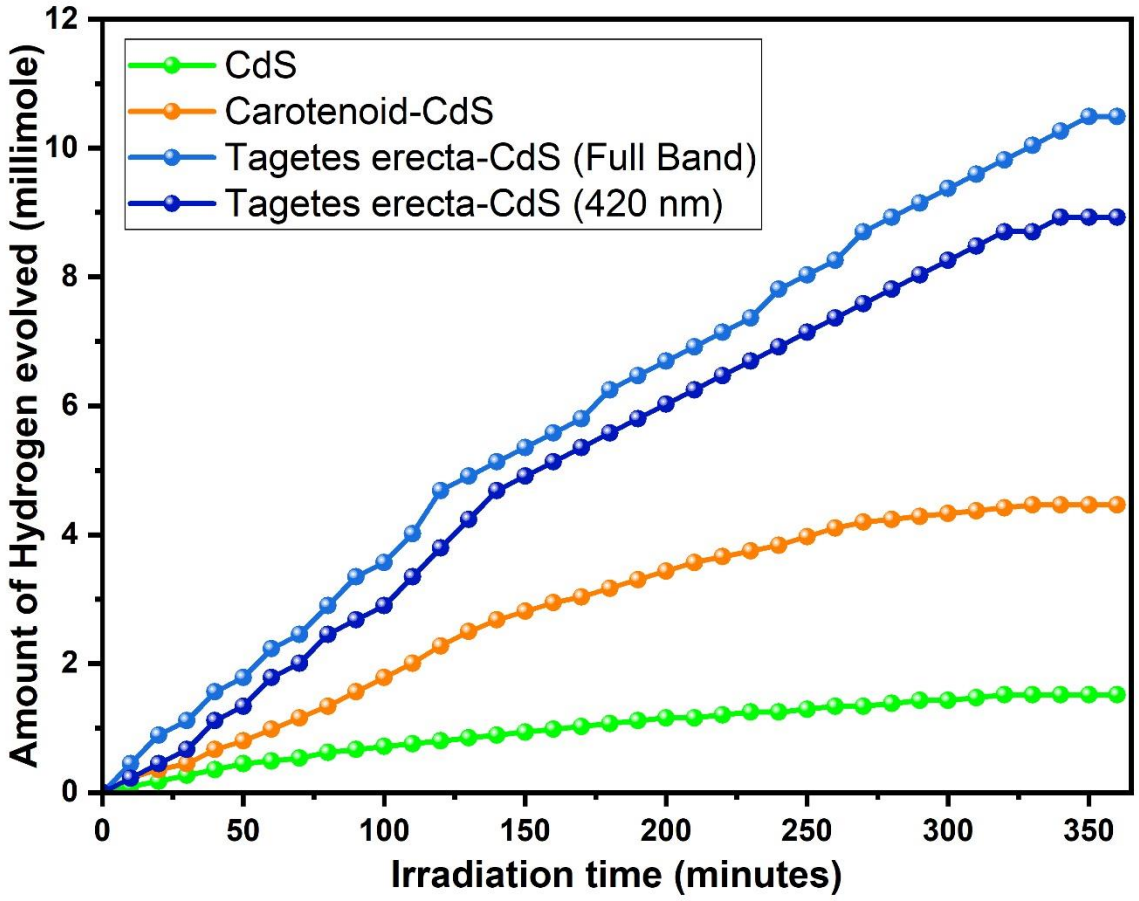


Fig 3.14: Amount of Hydrogen generated versus irradiation time using Cadmium sulfide, Carotenoid-CdS, and Tagetes erecta-CdS.

The performance of the Hydrogen generation by the photocatalytic water splitting was analysed using different photocatalyst system for 6 hours. The solar hydrogen generation using Tagetes erecta-CdS photocatalyst system shows high amount of Hydrogen generation (10.49 mmol) which was higher than Pristine CdS. CdS-Carotenoid shows intermediate Hydrogen generation performance in between CdS and Tagetes erecta-CdS photocatalyst system. The Tagetes erecta-CdS photocatalyst system shows the high performance in both UV and visible range due to the presence of organic pigment carotenoid and biomass. It has been observed that very low difference is obtained in between Tagetes erecta-CdS in full band and Tagetes erecta-CdS in UV range. This type of photocatalyst system were active in both UV and Visible range.

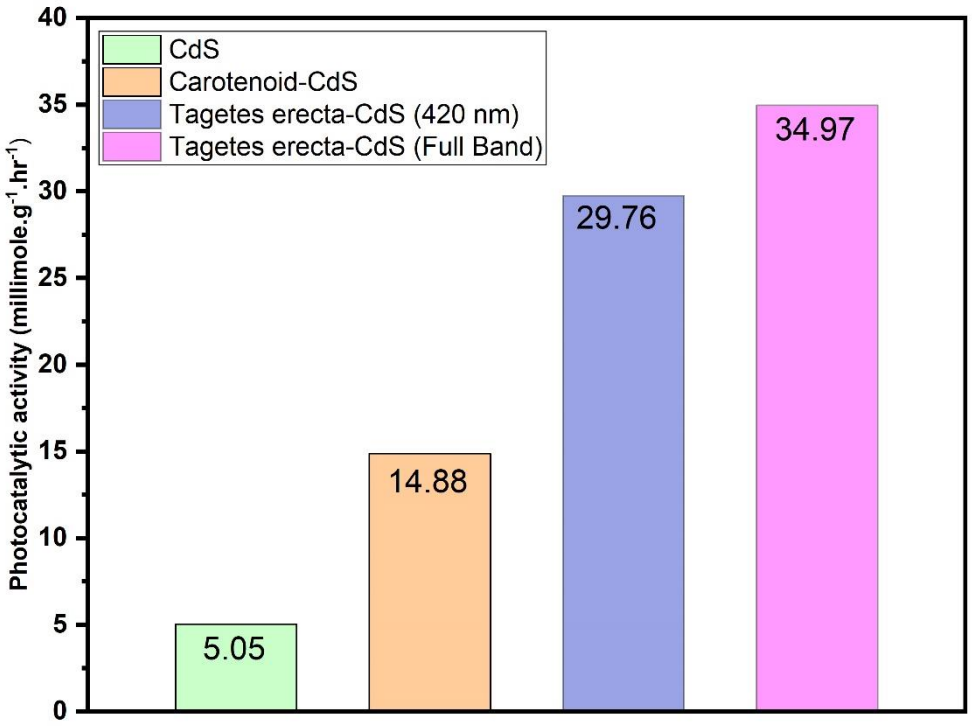


Fig 3.15: Photocatalytic activity comparison of different photocatalyst

Catalyst name	**Moles of Hydrogen generated (mmol) in 6 hrs**	**Photocatalytic activity ($mmol.g^{-1}.hr^{-1}$)**	**Average rate of hydrogen generation over 6 hrs mmol s^{-1}**	**STH efficiency**	**AQE (%)**
CdS	1.40	5.05	6.48×10^{-5} $mmol.s^{-1}$	1.22 %	------
Carotenoid-CdS	4.46	14.88	2.06×10^{-4} $mmol.s^{-1}$	3.90 %	------
Tagetes erecta-CdS (420 nm)	10.2	29.76	4.72×10^{-4} $mmol.s^{-1}$	8.93 %	17.25
Tagetes erecta-CdS (Full Band)	10.49	34.97	4.85×10^{-4} $mmol.s^{-1}$	9.17 %	------

Table 3.3: Millimoles of Hydrogen evolved, Photocatalytic activity, STH efficiency and AQE of CdS, Carotenoid-CdS, and Tagetes erecta-CdS.

Photocatalyst	Substrate	Activity ($mmol.h^{-1}.g.cat^{-1}$)	Reference
5% Pt/TiO2	Rice plant	0.058	[52]
5% Pt/TiO2	Chlorella algae	0.09	
0.5% Pt/TiO2	Alfalfa stems	0.10	
Co/CdS/CdOx	Sawdust	0.75	
Co/CdS/CdOx	Grass	1.0	
Co/CdS/CdOx	Bagasse	0.37	
Tagetes erecta-CdS	**Tagetes erecta**	**34.97**	**This work**

Table 3.4: Comparative analysis of Photocatalytic hydrogen production from raw biomass with synthesized photocatalyst.

3.5.1 Mechanism and Chemical reactions:

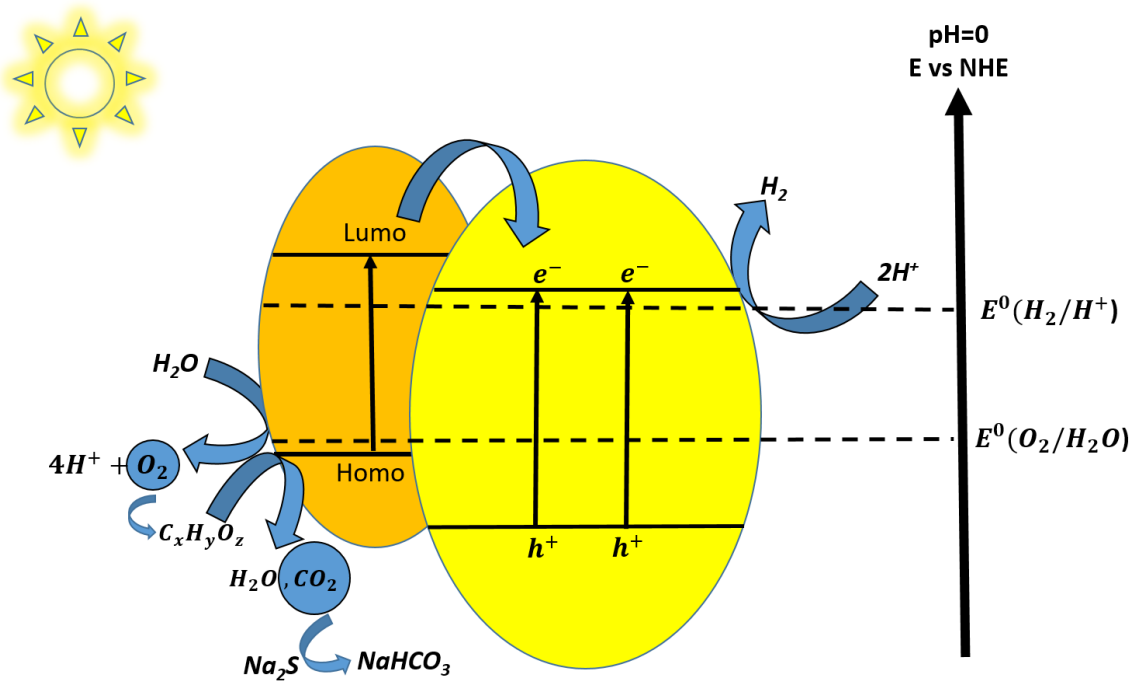


Fig 3.16: Mechanism of photocatalytic process.

3.5.2 Chemical reactions:

$$Carotenoid + h\nu \rightarrow Carotenoid^{*}$$ ----------(i)

$$CdS + h\nu \rightarrow CdS(h^{+}) + CdS(e^{-})$$ ----------(ii)

$$Carotenoid^{*} + CdS(h^{+}) \rightarrow Carotenoid^{+} + CdS$$----------(iii)

$$H_2O(l) + 2\,Carotenoid^{+} \rightarrow \frac{1}{2}\,O_2(g) + 2H^{+}$$----------(iv)

$$C_xH_yO_z + (2x - z)H_2O \rightarrow (2x + \frac{y}{2} - z)H_2 + xCO_2$$---------(v)

$$2CdS\,(e^{-}) + 2H^{+} \rightarrow CdS + H_2(g)$$----------(vi)

$$Carotenoid^{+} + \frac{1}{2}\,O_2 \rightarrow Carotenoid$$----------(vii)

$$Na_2S\,(s) + H_2O(l) + CO_2(g) \rightarrow NaHCO_3\,(aq)$$----------(viii)

3.6 Cost Analysis:

	Items	Amount Needed/Hours Used	Price in Rs. (INR)	Price in $ (USD)
Chemical used	Tap Water	2 L	-	-
	Tagetes erecta powder	0.1 g	-	-
	Deionized Water	60 ml	-	-
	Ethanol	100 ml	49.81	0.6000
	Cadmium Sulfide	0.1 g	5.99	0.0720
	Sodium Sulfide	0.01 g	0.0518	0.00062
Electricity used	Drying	23 hrs (2 kWh)	345	4.1300
	Centrifuge	0.25 hrs (1.6 kWh)	3.00	0.0360
	Hydrothermal	14 hr (2 kWh)	210.00	2.5100
	Vacuum Pump	0.25 hrs (0.0466 kWh)	0.0878	0.0011
	Stirring	6.5 hrs (1.17 kWh)	57.04	0.6800
	Solar Simulator	6 hrs (0.1 kWh)	4.5	0.0540

Total	**675.4796**	**8.09**

Table 3.5: Cost analysis of Hydrogen generation.

$$\boldsymbol{Cost = Instrument\ power\ consumption\ (kWh) * Time * unit\ cost}$$

- The estimated production cost of 10.49 mmol of hydrogen generation is $ 8.09.

Conclusion

Conclusions:

The hydrogen generation from synthesized photocatalyst using a photocatalytic method has a high capacity for conversion of solar irradiation energy and other renewable resources into potential chemicals as hydrogen. Tagetes erecta is utilized as a source of hydrogen which as a result only produces hydrogen and doesn't emit any kind of greenhouse gases. This work has been done using hydrothermally treated Tagetes erecta-CdS to generate high efficiency of hydrogen. The list of conclusions has been discussed below:

- The photocatalyst synthesized is more active in the UV range spectrum of solar irradiation because the absorption of photons is higher at 200-400 nm.

- The recorded photocatalytic activity of CdS and synthesized CdS-Tagetes erecta are **5.05 mmol.h^{-1}.g^{-1}** and **34.97 mmol.h^{-1}.g^{-1}** in which Tagetes erecta-CdS has a much higher hydrogen rate rather than CdS.

- From experimental findings AQY of Tagetes erecta-CdS is calculated at **420 nm** is **17.25 %.**

- Carotenoids present in Tagetes erecta-CdS act as a photon sensitizer which further transfers the excited electron to the CdS nanoparticle and charge separation efficiency increases. The time of recombination of electron-hole pairs increased which increased the photocatalytic activity of Tagetes erecta-CdS.

The estimated production cost of 10.49 mmol of hydrogen generation is $ 8.09.

Bibliography

[1] K. Aroh, “Globalization, Industralization and Population Growth the Fundamental Drivers of Pollution in a Given Society (India),” *SSRN Electron. J.*, no. January 2018, 2019, doi: 10.2139/ssrn.3453740.

[2] H. I. Abdel-Shafy and M. S. M. Mansour, “Solid waste issue: Sources, composition, disposal, recycling, and valorization,” *Egypt. J. Pet.*, vol. 27, no. 4, pp. 1275–1290, 2018, doi: 10.1016/j.ejpe.2018.07.003.

[3] C. C. dos Santos Accioly Lins, F. M. de Moraes Ramos-Perez, A. dos Anjos Pontual, M. L. dos Anjos Pontual, and E. H. L. do Nascimento, “Digital oral radiography,” *Digitization in Dentistry: Clinical Applications*. pp. 65–88, 2021. doi: 10.1007/978-3-030-65169-5_3.

[4] A. L. Srivastav and A. Kumar, “An endeavor to achieve sustainable development goals through floral waste management: A short review,” *J. Clean. Prod.*, vol. 283, p. 124669, 2021, doi: 10.1016/j.jclepro.2020.124669.

[5] A. Kumar Singhal, T. Gerito, D. Bedada, and O. Alemu ----------, “An Analysis of Micro Finance Institutions (With Respect To Loan Repayment),” *Int. J. Adv. Eng. Manag. (IJAEM*, vol. 2, no. 1, p. 1192, 2008, doi: 10.35629/5252-45122323.

[6] G. Elango and R. Govindasamy, “Analysis and utilization of temple waste flowers in Coimbatore District,” *Environ. Sci. Pollut. Res.*, vol. 25, no. 11, pp. 10688–10700, 2018, doi: 10.1007/s11356-018-1259-0.

[7] S. S. Soundarya, P. Radhika, D. S. Reddy, and K. Supriya, “An Analysis of Pattern of Floral Waste Generated and Disposal in Hyderabad City of Telangana State,” *Asian J. Agric. Extension, Econ. Sociol.*, no. December, pp. 414–420, 2021, doi: 10.9734/ajaees/2021/v39i1130768.

[8] P. K. Maity, “Impact of Waste Flower on Environment,” *Int. J. Res. Appl. Sci. Eng. Technol.*, no. August, 2016.

[9] “Pharma innovaton.pdf.”

[10] T. Demirbas and C. Demirbas, “Fuel Properties of Wood Species,” vol. 7036, 2009, doi: 10.1080/15567030802093153.

[11] B. Ramprakash, “Hydrogen Production from Wastewater by Biochemical Methods

Hydrogen Production from Wastewater by Biochemical Methods," no. September, 2020, doi: 10.1002/9781119300762.wsts0016.

[12] Y. S. H. Najjar, "Hydrogen safety : The road toward green technology," *Int. J. Hydrogen Energy*, vol. 38, no. 25, pp. 10716–10728, 2013, doi: 10.1016/j.ijhydene.2013.05.126.

[13] R. L. Germscheidt *et al.*, "Hydrogen Environmental Bene fi ts Depend on the Way of Production : An Overview of the Main Processes Production and Challenges by 2050," vol. 2100093, 2021, doi: 10.1002/aesr.202100093.

[14] A. Fujishima and K. Honda, "Electrochemical Evidence for the Mechanism of the Primary Stage of Photosynthesis," *Bull. Chem. Soc. Jpn.*, vol. 44, no. 4, pp. 1148–1150, Apr. 1971, doi: 10.1246/bcsj.44.1148.

[15] K. Shimura and H. Yoshida, "Heterogeneous photocatalytic hydrogen production from water and biomass derivatives," *Energy Environ. Sci.*, vol. 4, no. 7, pp. 2467–2481, 2011, doi: 10.1039/c1ee01120k.

[16] C. W. Huang, B. S. Nguyen, J. C. S. Wu, and V. H. Nguyen, "A current perspective for photocatalysis towards the hydrogen production from biomass-derived organic substances and water," *Int. J. Hydrogen Energy*, vol. 45, no. 36, pp. 18144–18159, 2020, doi: 10.1016/j.ijhydene.2019.08.121.

[17] K. A. Davis, S. Yoo, E. W. Shuler, B. D. Sherman, S. Lee, and G. Leem, "Photocatalytic hydrogen evolution from biomass conversion," *Nano Converg.*, vol. 8, no. 1, 2021, doi: 10.1186/s40580-021-00256-9.

[18] M. F. Kuehnel and E. Reisner, "Solar Hydrogen Generation from Lignocellulose," *Angew. Chemie - Int. Ed.*, vol. 57, no. 13, pp. 3290–3296, 2018, doi: 10.1002/anie.201710133.

[19] C. Bie, L. Wang, and J. Yu, "Challenges for photocatalytic overall water splitting," *Chem*, vol. 8, no. 6, pp. 1567–1574, 2022, doi: 10.1016/j.chempr.2022.04.013.

[20] D. Priyanka, T. Shalini, and V. Kumar Navneet, "A Brief Study on Marigold (Tagetes Species): a Review," *Int. Res. J. pharamacy*, vol. 4, no. 8, pp. 43–48, 2013.

[21] S. N. H. Jaafar, L. J. Minggu, K. Arifin, M. B. Kassim, and W. R. D. Wan, "Natural dyes as TIO2 sensitizers with membranes for photoelectrochemical water splitting: An overview," *Renew. Sustain. Energy Rev.*, vol. 78, no. February 2016, pp. 698–709, 2017,

doi: 10.1016/j.rser.2017.04.118.

[22] M. Butnariu, "Methods of Analysis (Extraction, Separation, Identification and Quantification) of Carotenoids from Natural Products," *J. Ecosyst. Ecography*, vol. 6, no. 2, 2016, doi: 10.4172/2157-7625.1000193.

[23] C. H. Park *et al.*, "Anthocyanin and carotenoid contents in different cultivars of chrysanthemum (dendranthema grandiflorum ramat.) flower," *Molecules*, vol. 20, no. 6, pp. 11090–11102, 2015, doi: 10.3390/molecules200611090.

[24] H. R. Akshaya, Namita, K. P. Singh, S. Saha, S. Panwar, and C. Bharadwaj, "Determination and correlation of carotenoid pigments and their antioxidant activities in marigold (Tagetes sp.) flowers," *Indian J. Agric. Sci.*, vol. 87, no. 3, pp. 390–396, 2017, doi: 10.56093/ijas.v87i3.68755.

[25] L. Fernandes, E. Ramalhosa, J. A. Pereira, J. A. Saraiva, and S. Casal, "The unexplored potential of edible flowers lipids," *Agric.*, vol. 8, no. 10, pp. 1–23, 2018, doi: 10.3390/agriculture8100146.

[26] A. Ninčević Grassino, S. Rimac Brnčić, M. Badanjak Sabolović, J. Šic Žlabur, R. Marović, and M. Brnčić, "Carotenoid Content and Profiles of Pumpkin Products and By-Products," *Molecules*, vol. 28, no. 2, 2023, doi: 10.3390/molecules28020858.

[27] Y. Murakami, Y. Fukui, H. Watanabe, H. Kokubun, Y. Toya, and T. Ando, "Distribution of carotenoids in the flower of non-yellow commercial petunia," *J. Hortic. Sci. Biotechnol.*, vol. 78, no. 2, pp. 127–130, Jan. 2003, doi: 10.1080/14620316.2003.11511594.

[28] R. S. Kapadnis *et al.*, "Cadmium Telluride/Cadmium Sulfide Thin Films Solar Cells: A Review," *ES Energy Environ.*, vol. 10, pp. 3–12, 2020, doi: 10.30919/esee8c706.

[29] A. Kudo and Y. Miseki, "Heterogeneous photocatalyst materials for water splitting," *Chem. Soc. Rev.*, vol. 38, no. 1, pp. 253–278, 2009, doi: 10.1039/b800489g.

[30] V. Singh and P. Chauhan, "Synthesis and structural properties of wurtzite type cds nanoparticles," *Chalcogenide Lett.*, vol. 6, no. 9, pp. 421–426, 2009.

[31] M. J. Pawar and S. S. Chaure, "Synthesis of cds nanoparticles using glucose as a capping agent," *Chalcogenide Lett.*, vol. 6, no. 12, pp. 689–693, 2009.

[32] S. Sharma, V. Dutta, P. Raizada, A. Hosseini-Bandegharaei, P. Singh, and V. H. Nguyen, *Tailoring cadmium sulfide-based photocatalytic nanomaterials for water decontamination: a review*, vol. 19, no. 1. Springer International Publishing, 2021. doi: 10.1007/s10311-020-01066-x.

[33] Y. J. Yuan, D. Chen, Z. T. Yu, and Z. G. Zou, "Cadmium sulfide-based nanomaterials for photocatalytic hydrogen production," *J. Mater. Chem. A*, vol. 6, no. 25, pp. 11606–11630, 2018, doi: 10.1039/c8ta00671g.

[34] N. Kamarulzaman, M. F. Kasim, and N. F. Chayed, "Elucidation of the highest valence band and lowest conduction band shifts using XPS for ZnO and Zn0.99Cu0.01O band gap changes," *Results Phys.*, vol. 6, no. April, pp. 217–230, 2016, doi: 10.1016/j.rinp.2016.04.001.

[35] P. Makuła, M. Pacia, and W. Macyk, "How To Correctly Determine the Band Gap Energy of Modified Semiconductor Photocatalysts Based on UV-Vis Spectra," *J. Phys. Chem. Lett.*, vol. 9, no. 23, pp. 6814–6817, 2018, doi: 10.1021/acs.jpclett.8b02892.

[36] I. M. Mehedi, A. Im, S. Islam, H. Shah, V. Shrotriya, and M. B. Zaman, "Rapid one pot syntheses of magnetic Zn 1-x Fe x S nanostructures : Enhancing properties of ZnS material for effective photocatalytic application," *Ceram. Int.*, vol. 50, no. 9PB, pp. 16131–16141, 2024, doi: 10.1016/j.ceramint.2024.02.093.

[37] A. Ali, "X-ray Diffraction Techniques for Mineral Characterization : A Review for Engineers of the Fundamentals , Applications , and Research Directions," 2022.

[38] R. Paper and B. A. Measurement, "Michael HART," vol. 55, 1981.

[39] M. A. Mohamed, J. Jaafar, A. F. Ismail, M. H. D. Othman, and M. A. Rahman, *Spectroscopy*. Elsevier B.V., 2017. doi: 10.1016/B978-0-444-63776-5.00001-2.

[40] T. Analysis, "TGA 4000 Thermogravimetric Analyzer".

[41] K. Mikroskop, E. Imbasan, P. Medan, and D. I. Bti, "Field emission scanning electron microscope (fe-sem) facility in bti".

[42] C. R. Mcneill, I. Hwang, and N. C. Greenham, "Photocurrent transients in all-polymer solar cells: Trapping and detrapping effects ," vol. 024507, 2009, doi: 10.1063/1.3177337.

[43] “Derioation We consider the simple electrode reaction , R ~ O + ne , that occurs at the,” vol. 171, pp. 219–230, 1984.

[44] K. J. Rountree, B. D. Mccarthy, E. S. Rountree, T. T. Eisenhart, and J. L. Dempsey, “A Practical Beginner ’ s Guide to Cyclic Voltammetry,” 2017, doi: 10.1021/acs.jchemed.7b00361.

[45] W. Mäntele and E. Deniz, “Spectrochimica Acta Part A : Molecular and Biomolecular Spectroscopy UV – VIS absorption spectroscopy : Lambert-Beer reloaded,” *SAA*, vol. 173, pp. 965–968, 2017, doi: 10.1016/j.saa.2016.09.037.

[46] A. Gao, P. J. Rizo, L. Scaccabarozzi, C. J. Lee, V. Banine, and F. Bijkerk, “Photoluminescence-based detection of particle contamination on extreme ultraviolet reticles,” 2015, doi: 10.1063/1.4922883.

[47] A. Gao, P. J. Rizo, L. Scaccabarozzi, C. J. Lee, V. Banine, and F. Bijkerk, “Photoluminescence-based detection of particle contamination on extreme ultraviolet reticles,” *Rev. Sci. Instrum.*, vol. 86, no. 6, 2015, doi: 10.1063/1.4922883.

[48] T. Lcs-, S. S. Simulators, C. Abb, and S. Simulators, “LCS-100 Series Small Area Solar Simulators,” pp. 2–5.

[49] A. Sarkar, M. Kumar, S. Das, and S. Mandal, “Facile in-situ synthesis of solid mediator based CdS-rGO-WO 3 Z-scheme photocatalytic system for efficient photocatalytic hydrogen generation,” *Opt. Mater. (Amst).*, vol. 147, no. December 2023, p. 114670, 2024, doi: 10.1016/j.optmat.2023.114670.

[50] M. Xu, Y. Kang, L. Jiang, L. Jiang, P. L. Tremblay, and T. Zhang, “The one-step hydrothermal synthesis of CdS nanorods modified with carbonized leaves from Japanese raisin trees for photocatalytic hydrogen evolution,” *Int. J. Hydrogen Energy*, vol. 47, no. 34, pp. 15516–15527, 2022, doi: 10.1016/j.ijhydene.2021.09.023.

[51] S. Thanikaikarasan, T. Mahalingam, M. Raja, and S. Velumani, “Electrochemical growth and characterization of iron doped cadmium sulfide thin films,” *Mater. Sci. Semicond. Process.*, vol. 37, pp. 215–222, 2015, doi: 10.1016/j.mssp.2015.03.017.

[52] D. W. Wakerley, M. F. Kuehnel, K. L. Orchard, K. H. Ly, T. E. Rosser, and E. Reisner, “Solar-driven reforming of lignocellulose to H2 with a CdS/CdOx photocatalyst,” *Nat. Energy*, vol. 2, no. 4, pp. 1–9, 2017, doi: 10.1038/nenergy.2017.21.